
Project JRP — Lattice QCD Calculations

Harvey Meyer and Hartmut Wittig

Institute for Nuclear Physics, Helmholtz Institute Mainz, and PRISMA⁺ Cluster of Excellence,
Johannes Gutenberg-Universität Mainz

FOR5237 Workshop

Schloss Rheinfels, St. Goar

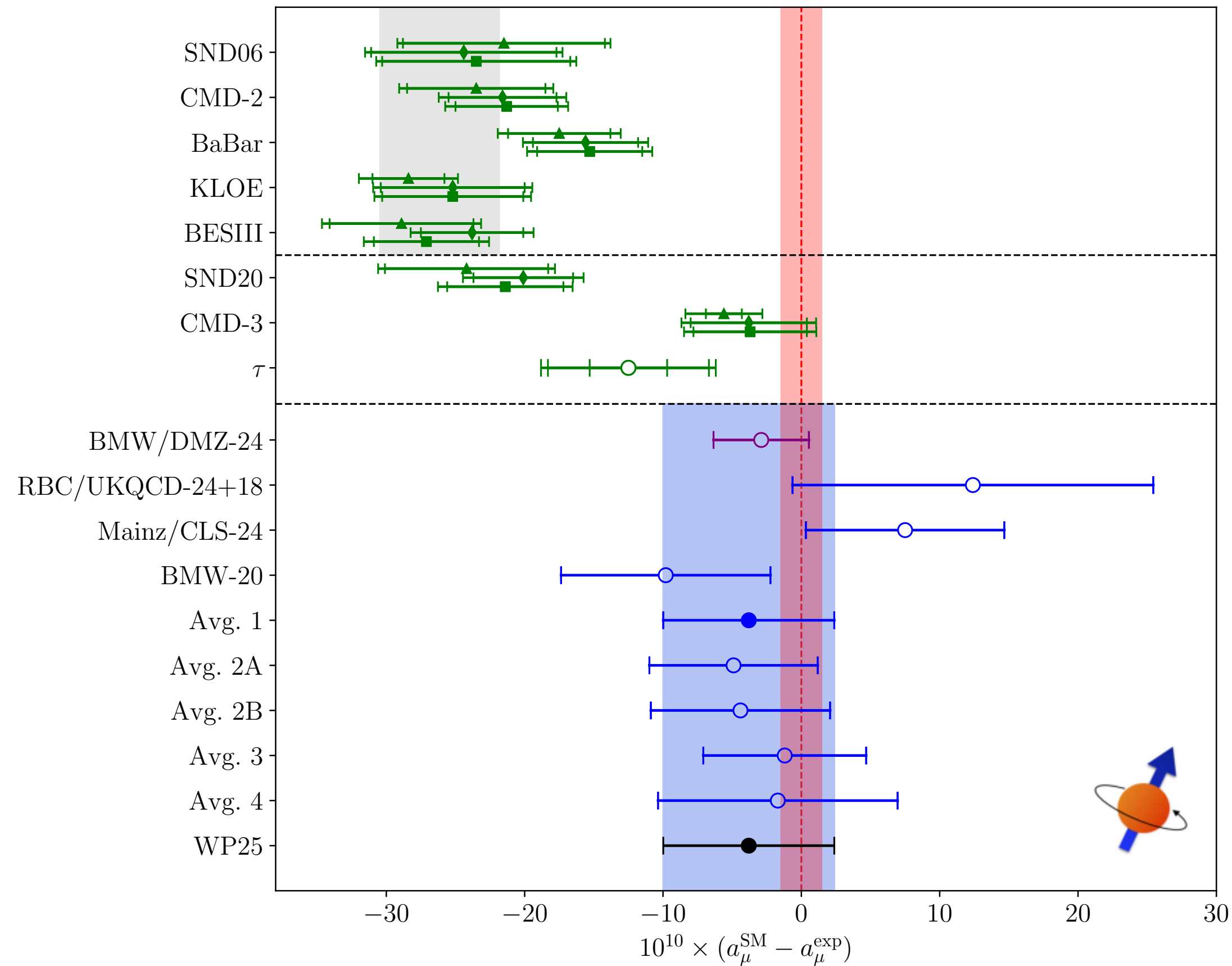
11–13 June 2024



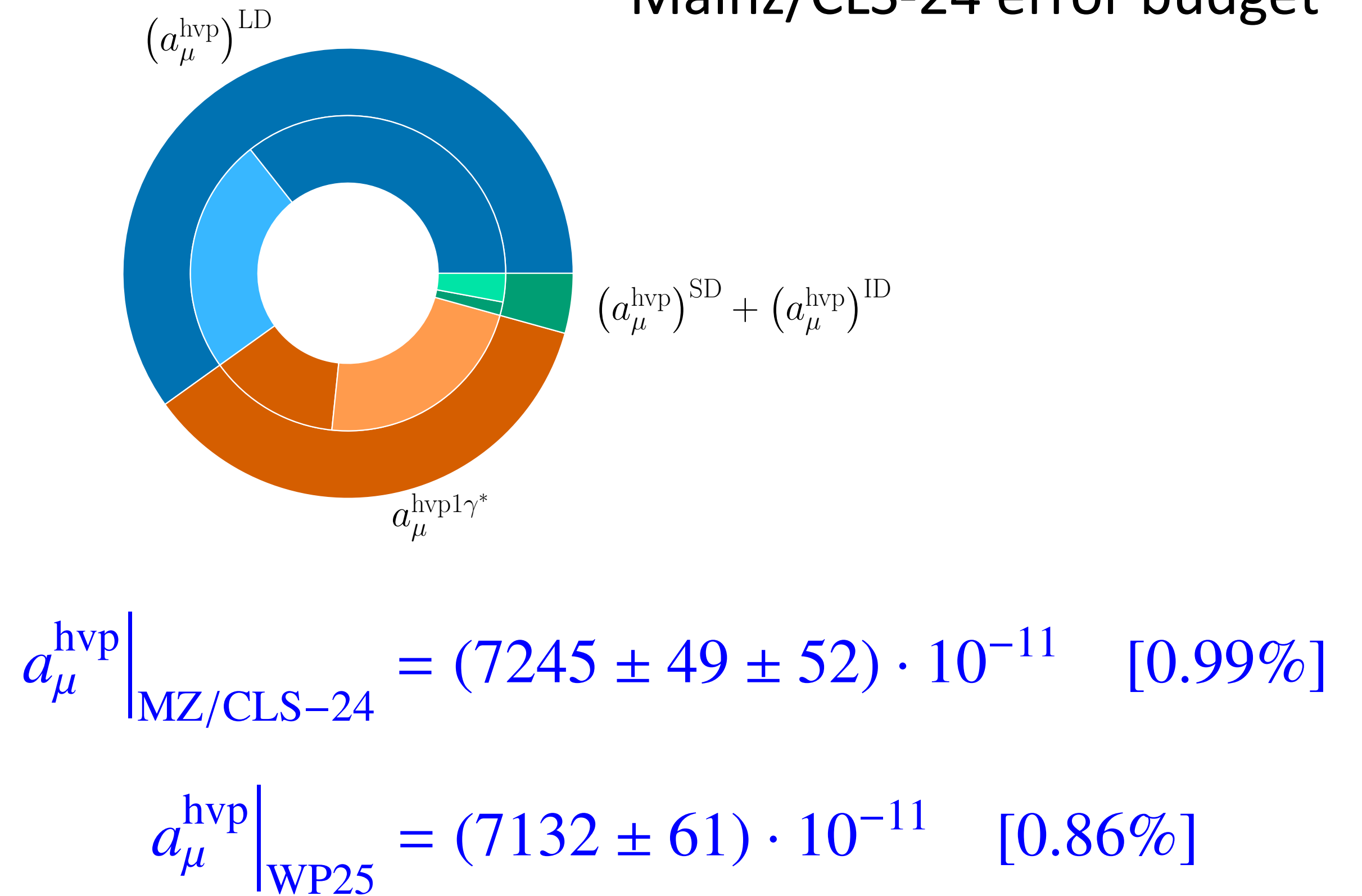
JOHANNES GUTENBERG
UNIVERSITÄT MAINZ



Muon $g - 2$ after WP25 and E989



Mainz/CLS-24 error budget



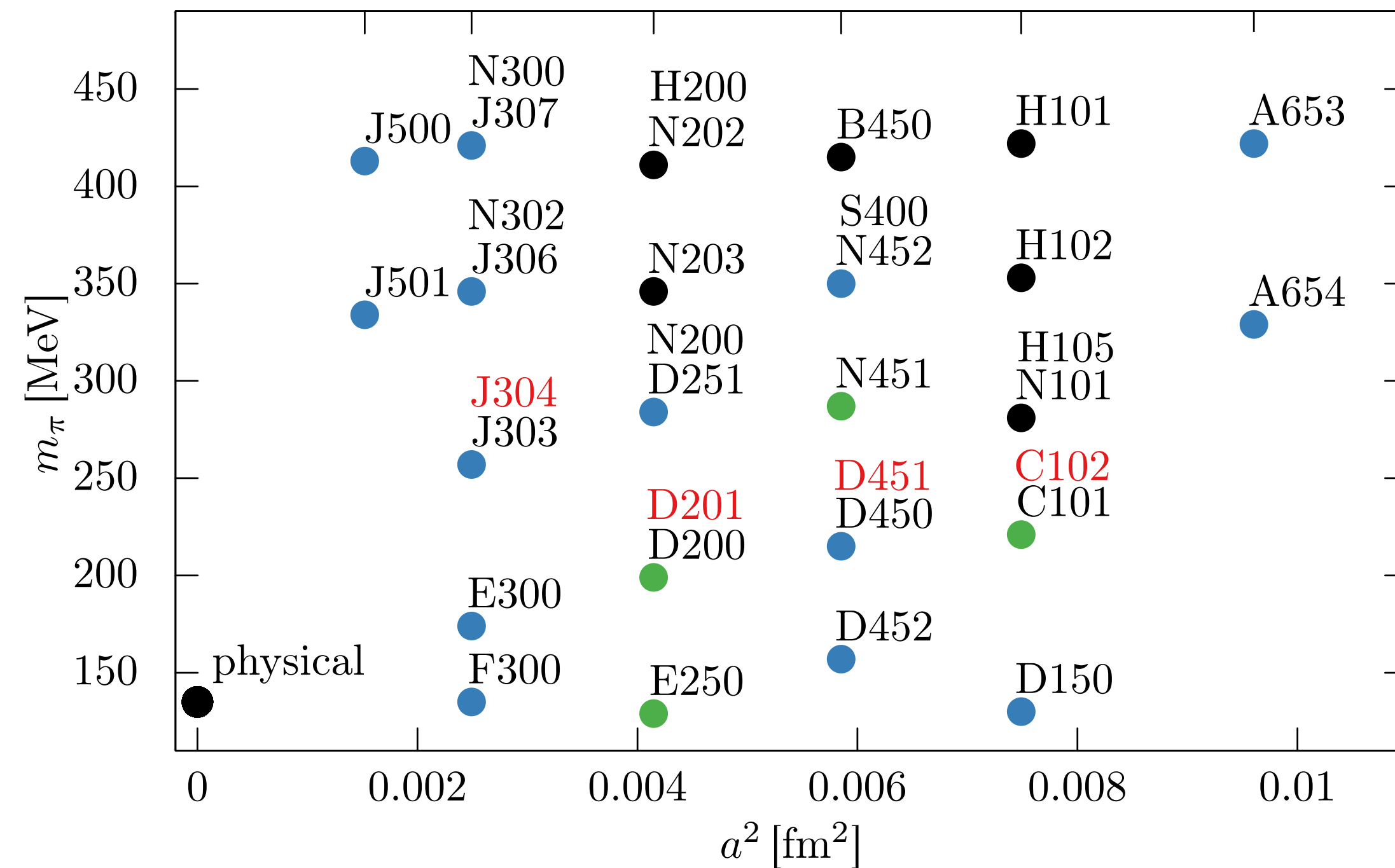
Statistical precision of isovector contribution and isospin-breaking effects dominate error

[Aliberti et al., arXiv:2505.21476; Djukanovic et al., JHEP 04 (2025) 098]

Lattice QCD at Mainz

Ensembles with $N_f = 2 + 1$ flavours of $O(a)$ improved Wilson fermions generated by CLS effort

Six lattice spacings: $a = 0.099 - 0.035$ fm; Pion masses: $m_\pi = 130 - 420$ MeV



Computational cost: ≈ 400 M core-hrs

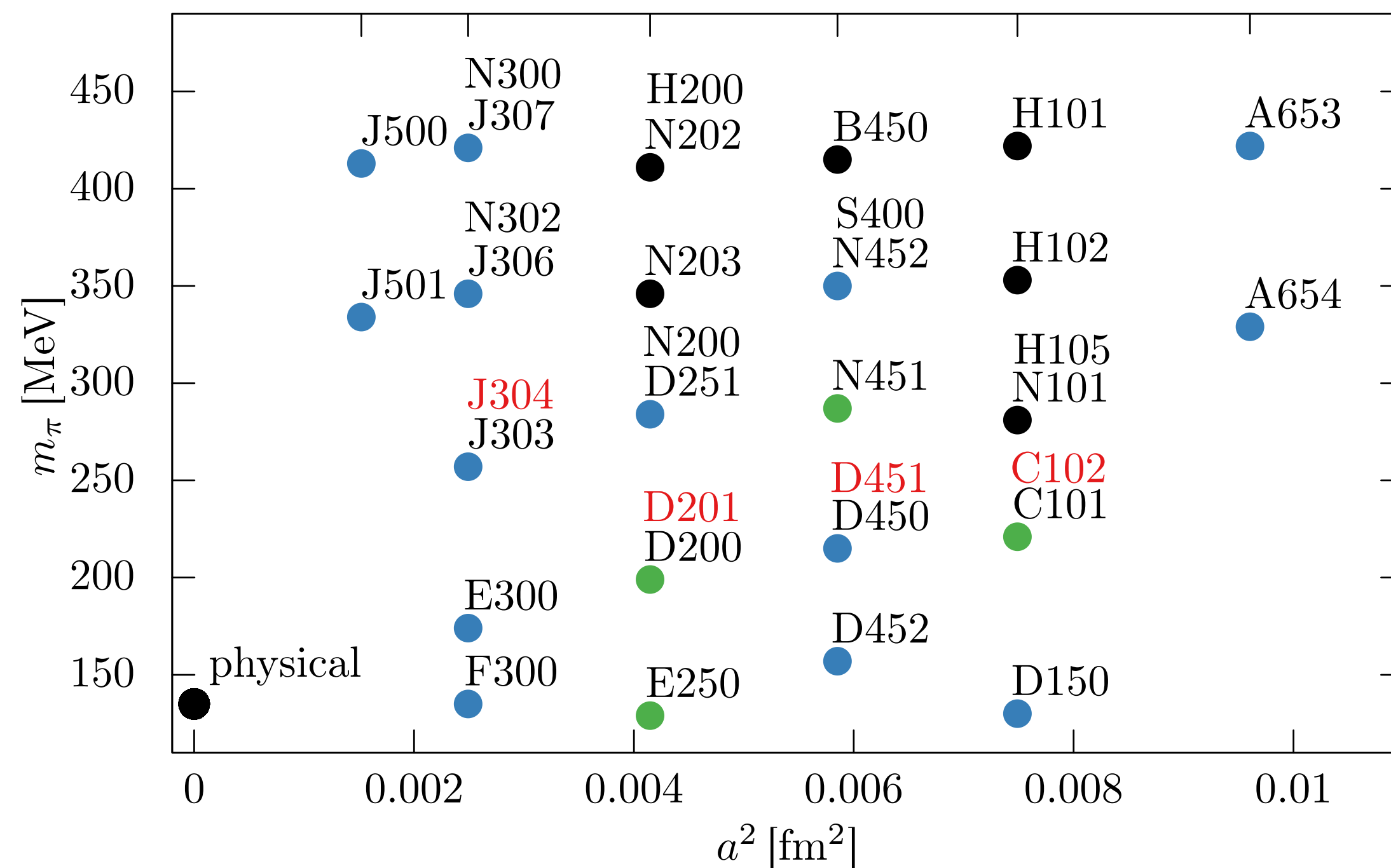
Ensemble “F300”:

$$m_\pi \approx 135 \text{ MeV}, \quad a = 0.050 \text{ fm}, \quad 128^3 \cdot 256$$

Lattice QCD at Mainz

Ensembles with $N_f = 2 + 1$ flavours of $O(a)$ improved Wilson fermions generated by CLS effort

Six lattice spacings: $a = 0.099 - 0.035$ fm; Pion masses: $m_\pi = 130 - 420$ MeV



Computational cost: ≈ 400 M core-hrs p.a.

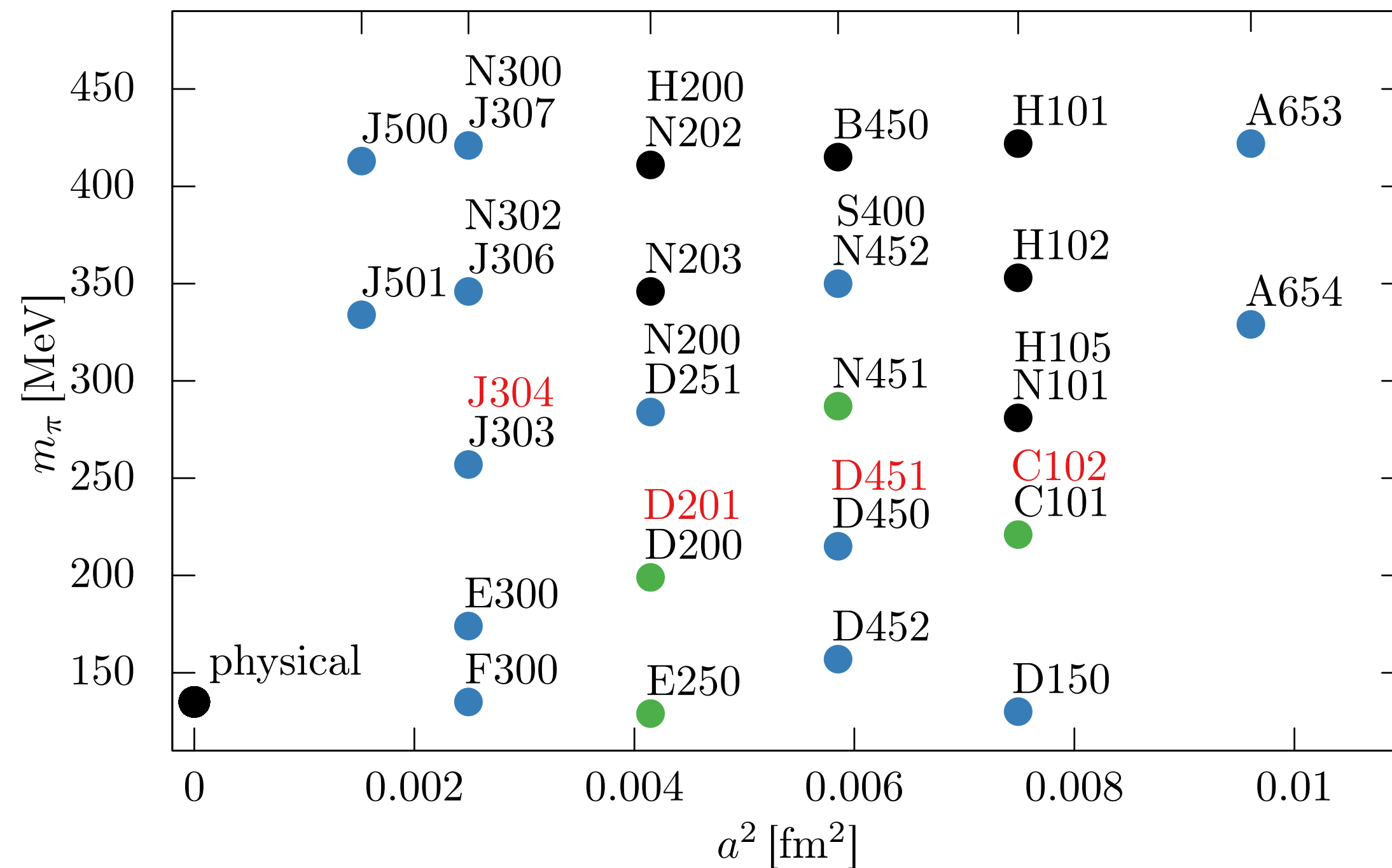
Ensemble “F300”:

$$m_\pi \approx 135 \text{ MeV}, \quad a = 0.050 \text{ fm}, \quad 128^3 \cdot 256$$

Lattice QCD at Mainz

Ensembles with $N_f = 2 + 1$ flavours of $O(a)$ improved Wilson fermions generated by CLS effort

Six lattice spacings: $a = 0.099 - 0.035$ fm; Pion masses: $m_\pi = 130 - 420$ MeV



Computational cost: ≈ 400 M core-hrs p.a.

Intrinsic numerical cost

Wilson fermions



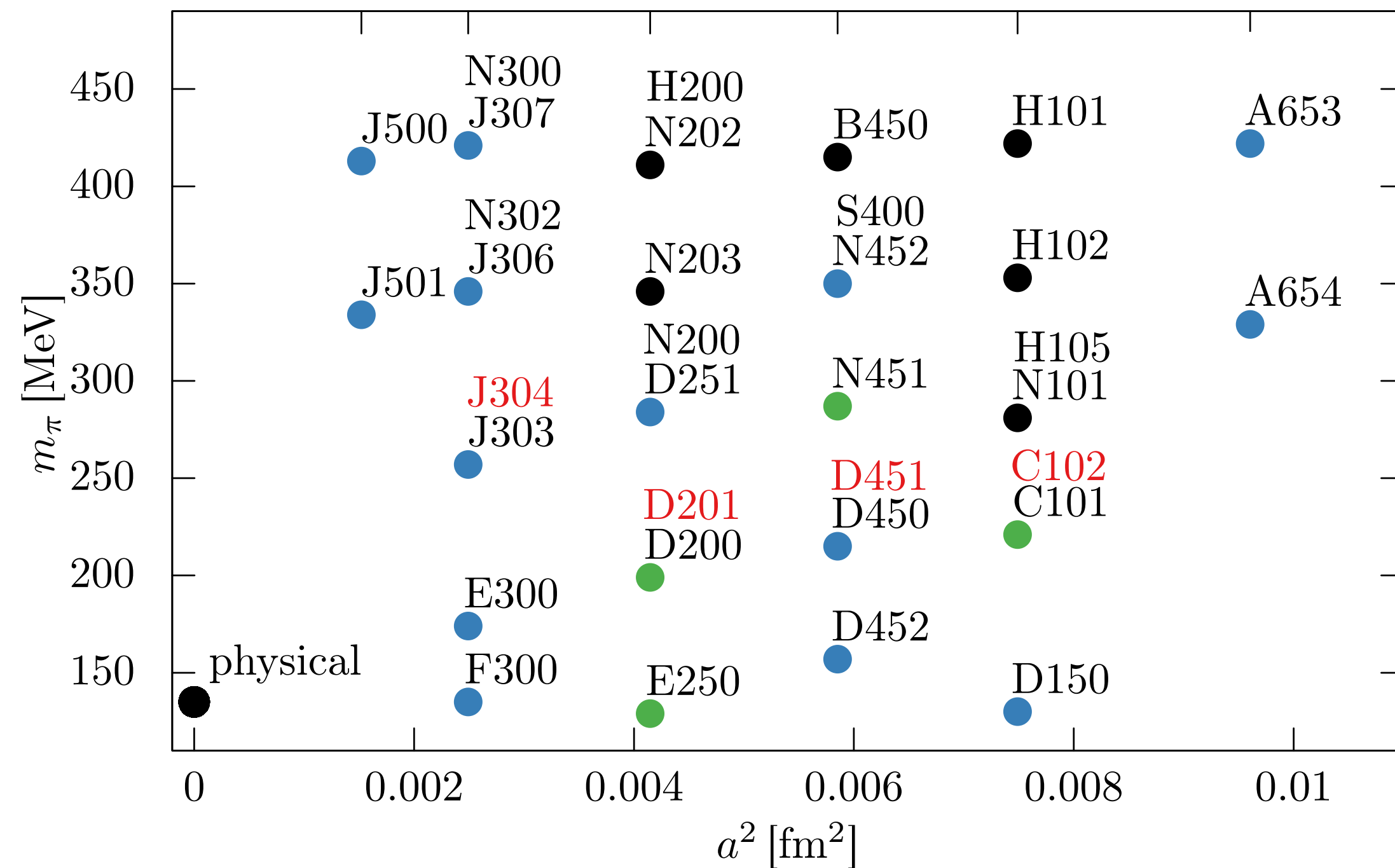
Ensemble "F300":

$$m_\pi \approx 135 \text{ MeV}, \quad a = 0.050 \text{ fm}, \quad 128^3 \cdot 256$$

Lattice QCD at Mainz

Ensembles with $N_f = 2 + 1$ flavours of $O(a)$ improved Wilson fermions generated by CLS effort

Six lattice spacings: $a = 0.099 - 0.035$ fm; Pion masses: $m_\pi = 130 - 420$ MeV

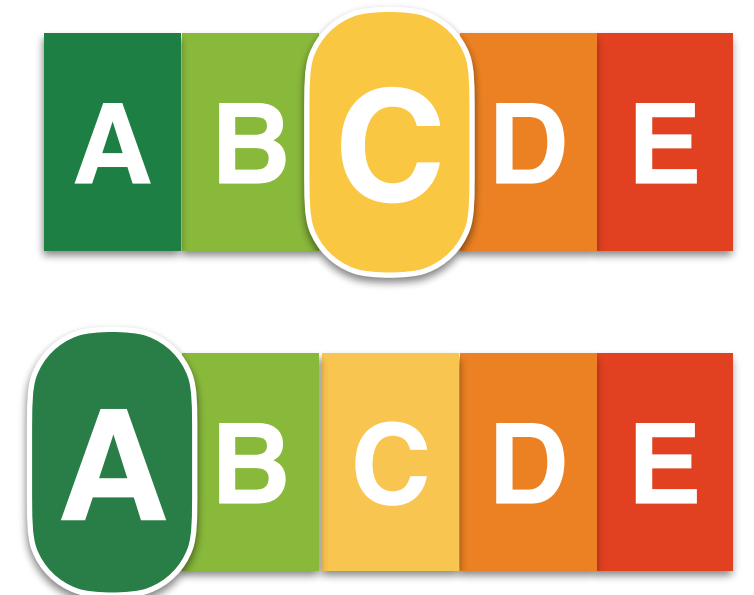


Computational cost: ≈ 400 M core-hrs p.a.

Intrinsic numerical cost

Wilson fermions

Staggered fermions



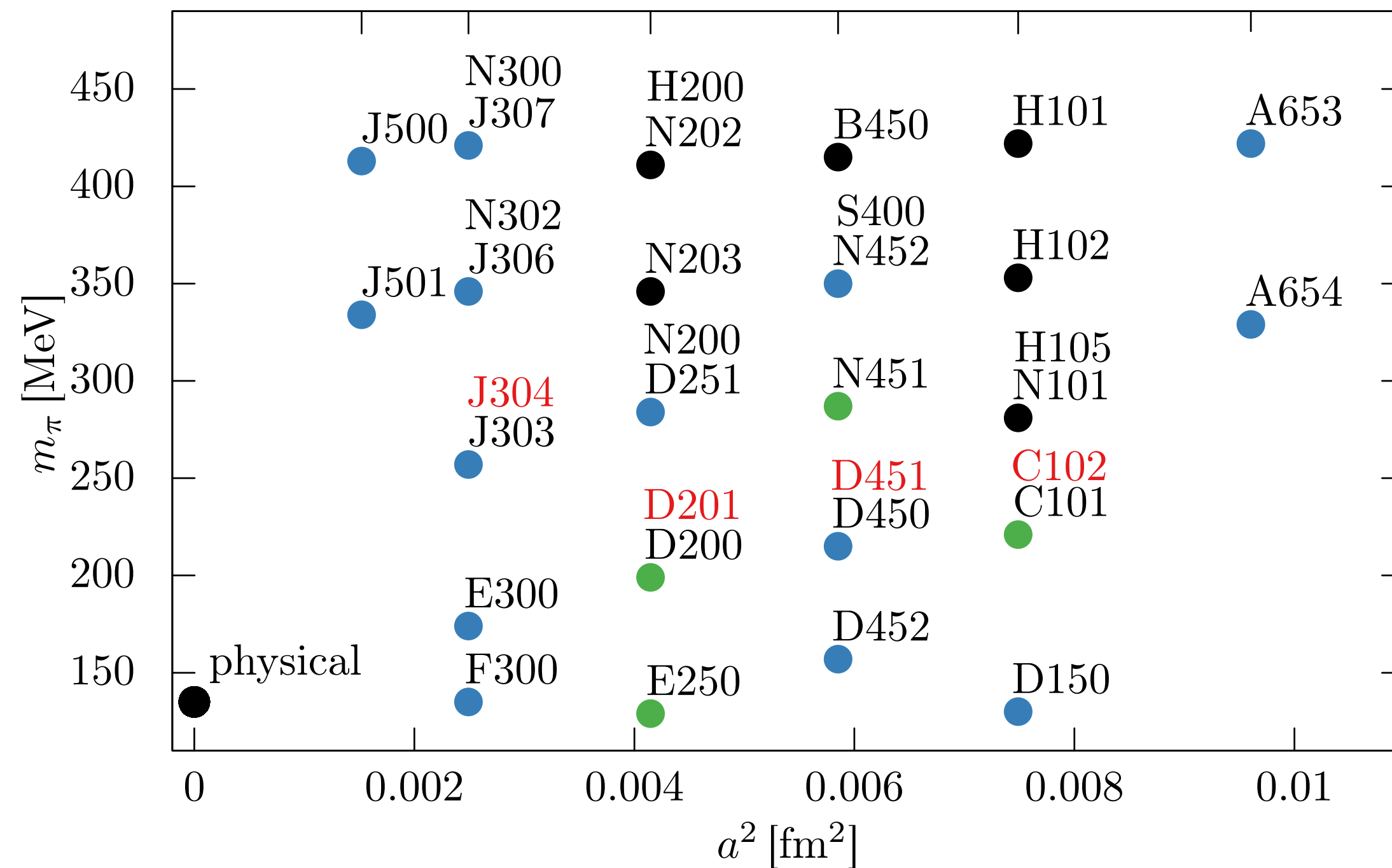
Ensemble “F300”:

$$m_\pi \approx 135 \text{ MeV}, \quad a = 0.050 \text{ fm}, \quad 128^3 \cdot 256$$

Lattice QCD at Mainz

Ensembles with $N_f = 2 + 1$ flavours of $O(a)$ improved Wilson fermions generated by CLS effort

Six lattice spacings: $a = 0.099 - 0.035$ fm; Pion masses: $m_\pi = 130 - 420$ MeV



Computational cost: ≈ 400 M core-hrs p.a.

Intrinsic numerical cost

Wilson fermions



Staggered fermions



Domain-wall fermions



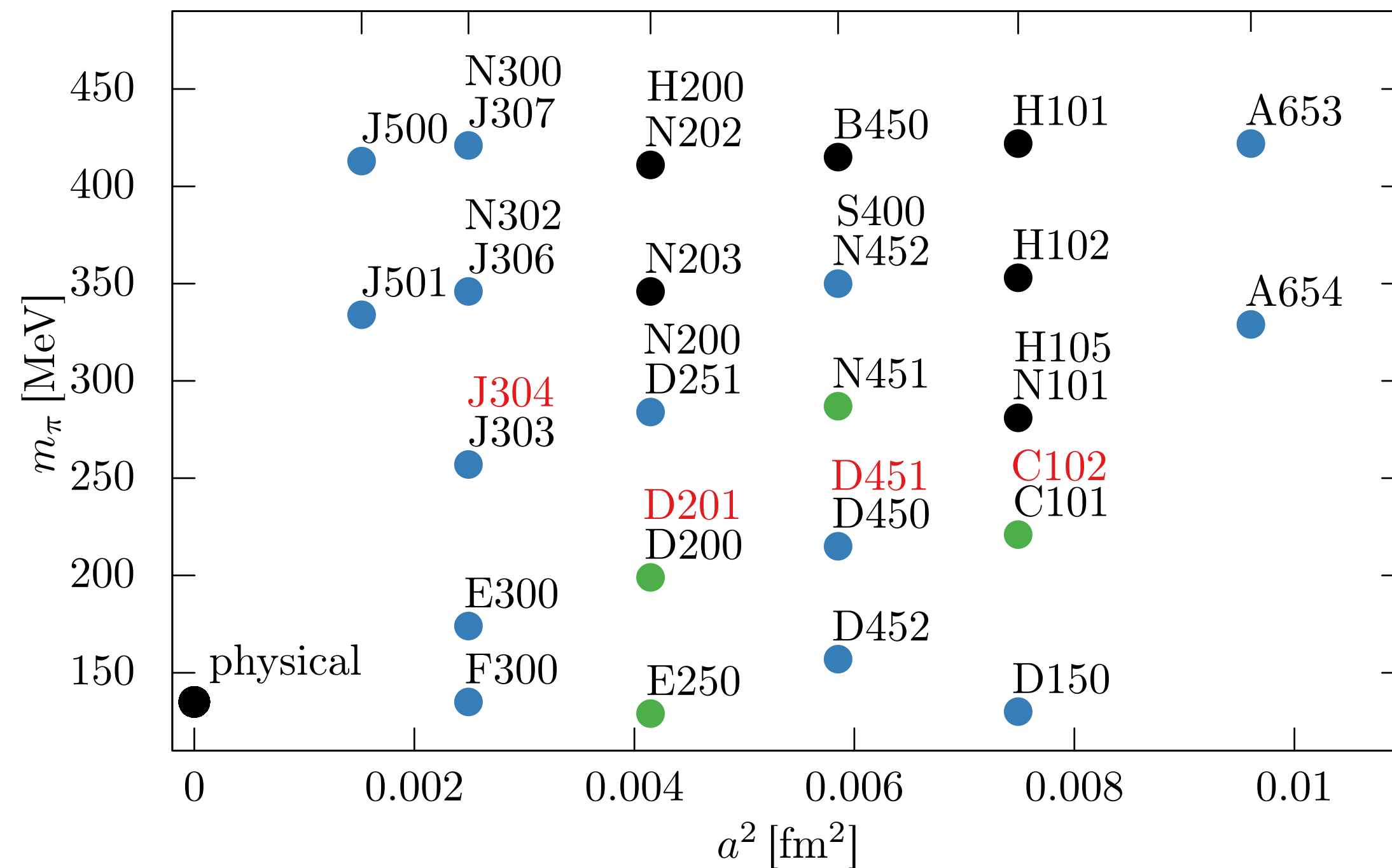
Ensemble “F300”:

$$m_\pi \approx 135 \text{ MeV}, \quad a = 0.050 \text{ fm}, \quad 128^3 \cdot 256$$

Lattice QCD at Mainz

Ensembles with $N_f = 2 + 1$ flavours of $O(a)$ improved Wilson fermions generated by CLS effort

Six lattice spacings: $a = 0.099 - 0.035$ fm; Pion masses: $m_\pi = 130 - 420$ MeV



Ensemble “F300”:

$$m_\pi \approx 135 \text{ MeV}, \quad a = 0.050 \text{ fm}, \quad 128^3 \cdot 256$$

Computational cost: ≈ 400 M core-hrs p.a.

Conceptual issues / fermion doubling problem

Wilson fermions



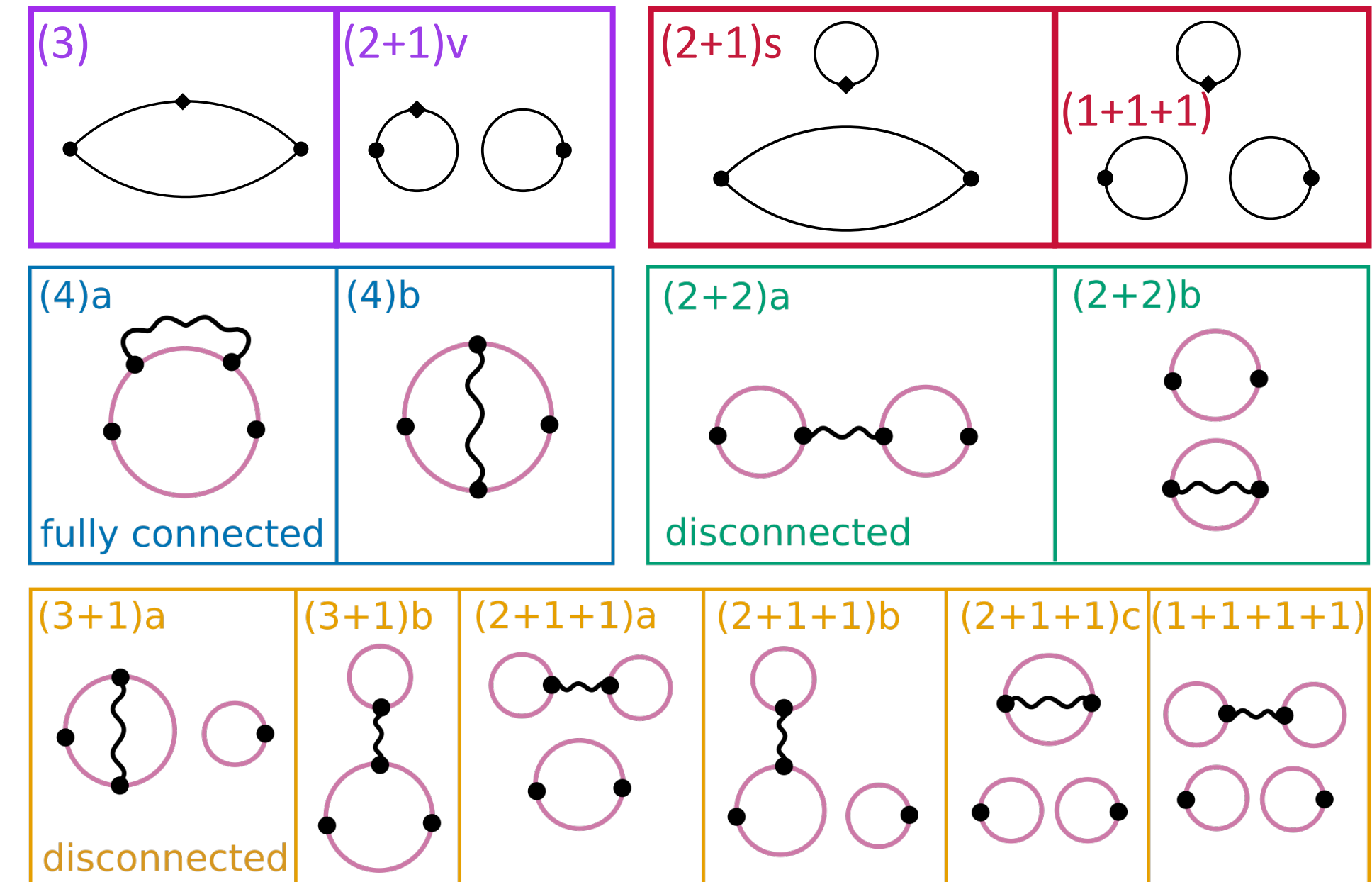
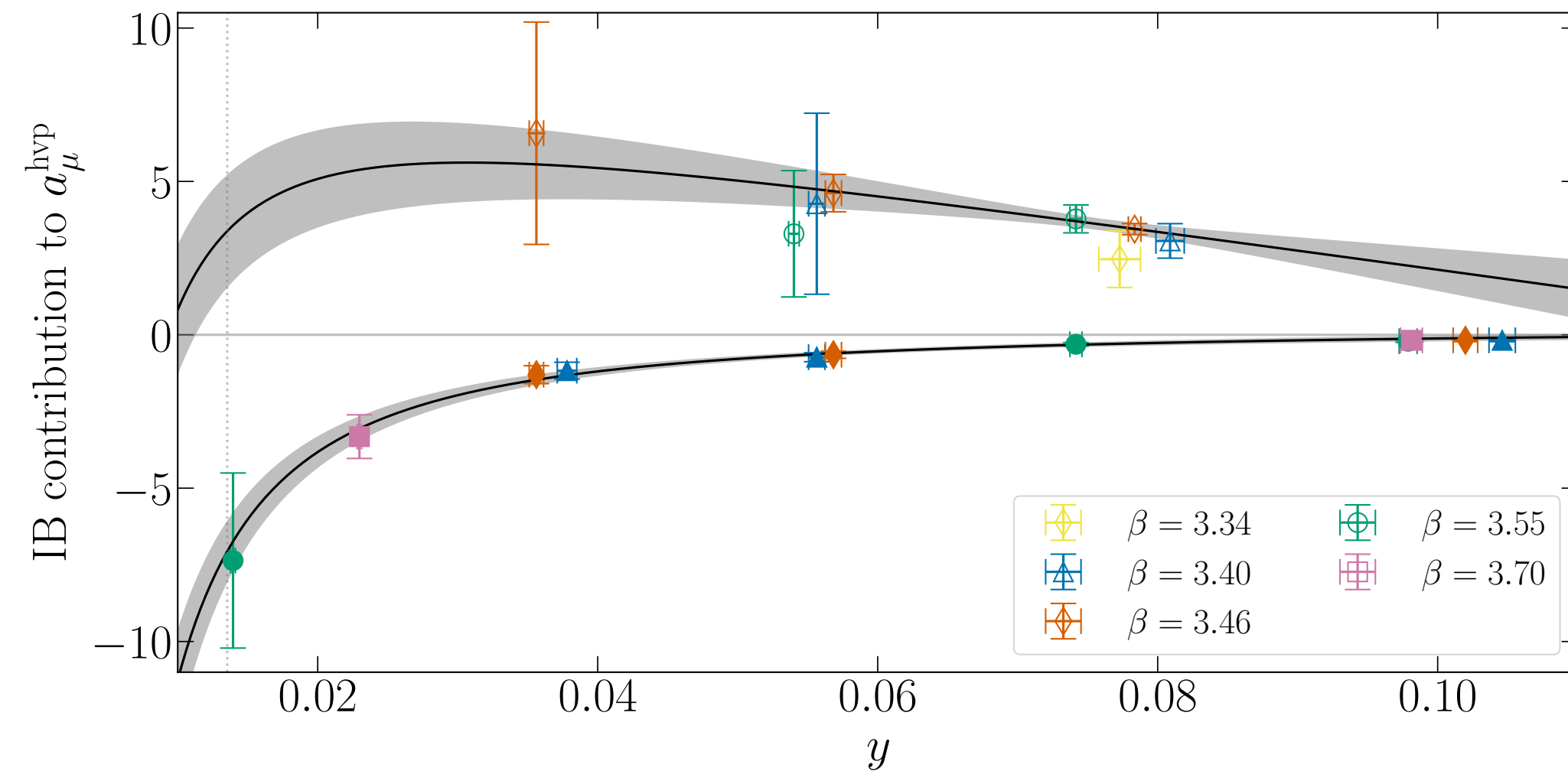
Staggered fermions



Domain-wall fermions



Isospin-breaking corrections in Mainz/CLS-24



Upper curve: (3) + (4)a + (4)b + ChPT-estimate of (2+1)v; “Rome approach” and QED_L

Lower curve: (2+2)a; photon propagator in continuum and infinite volume; remaining diagrams estimated via charged pion loop

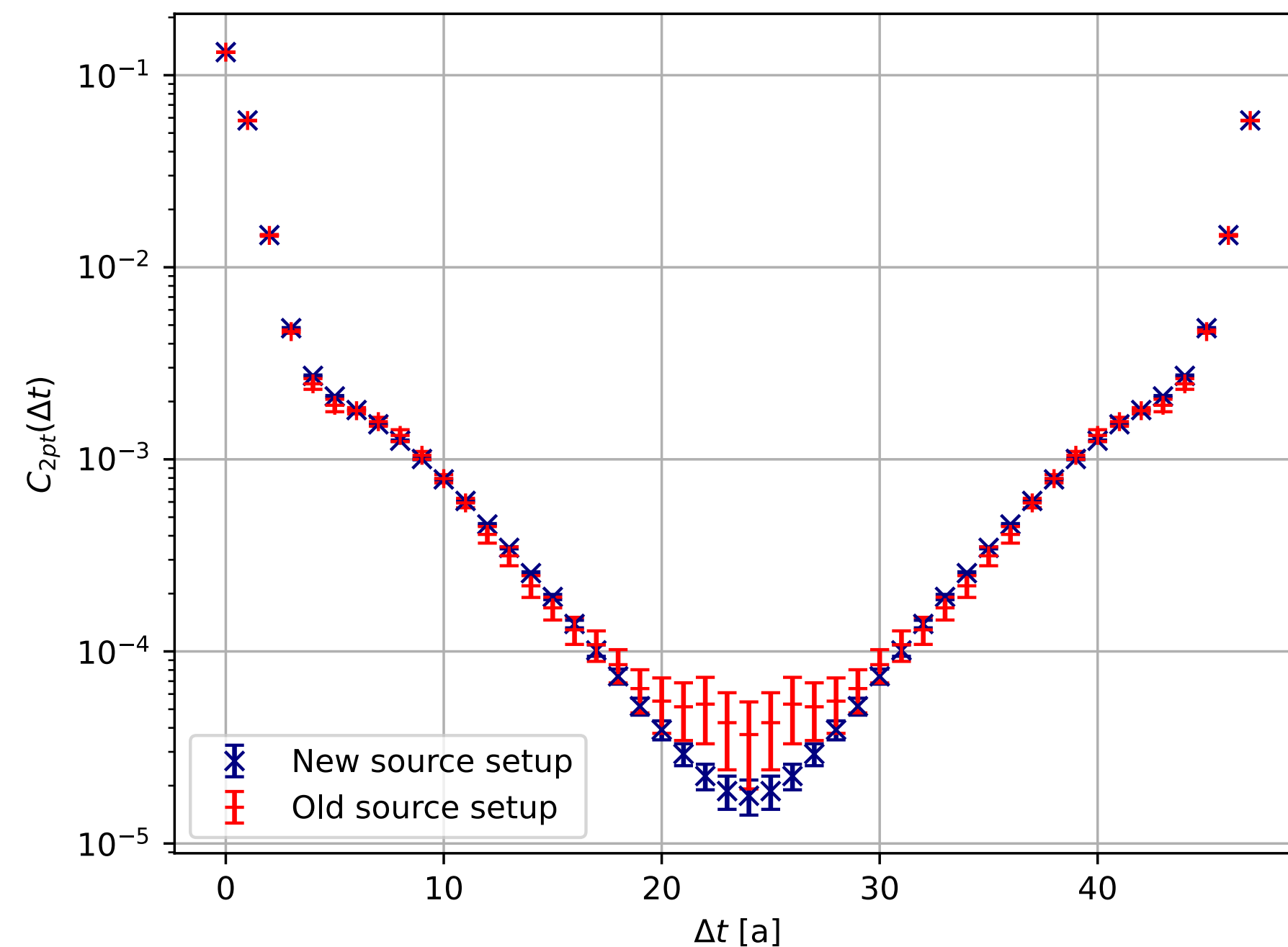
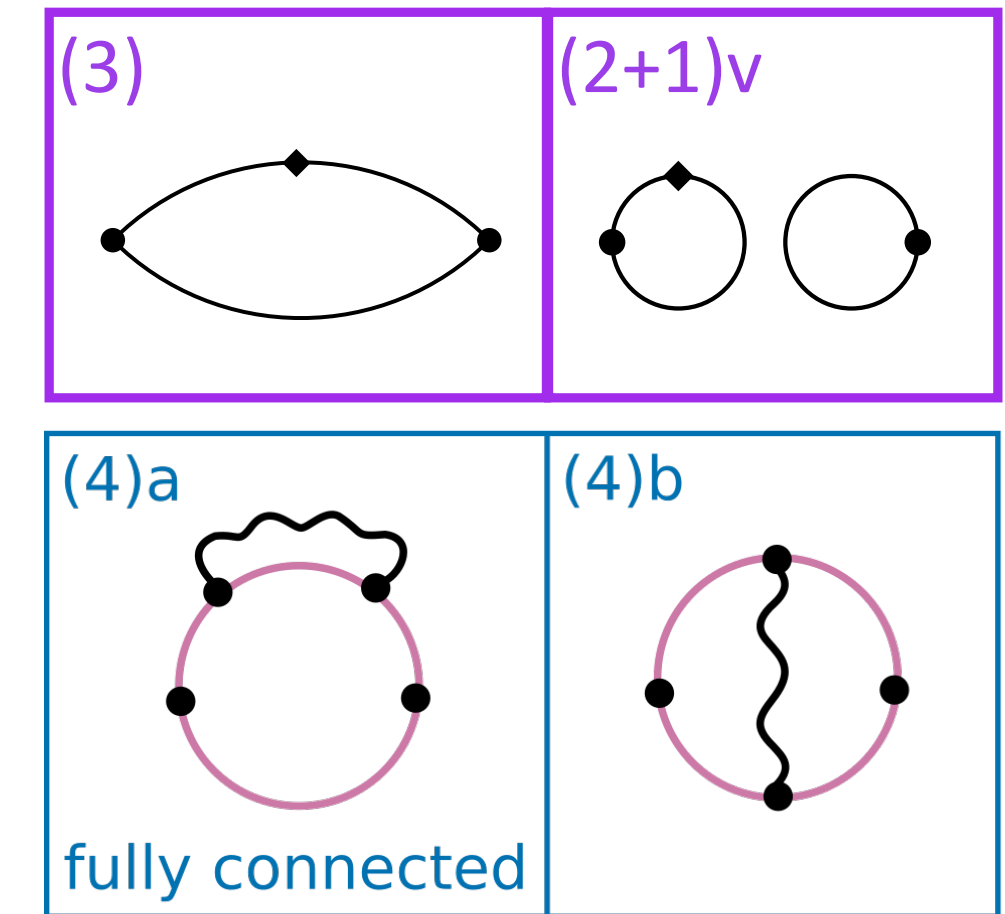
$$a_{\mu}^{\text{hvp}} \Big|_{\text{IB}} \cdot 10^{11} = -(41 \pm 24 \pm 9 \pm 35)[\pm 43]$$

[Djukanovic et al., JHEP 04 (2025) 098; Parrino et al., arXiv:2501.03192]

Isospin-breaking effects

Combat high levels of statistical noise in evaluation of mass insertion and fully connected QED diagrams using “Rome approach” and QED_L

- Low-mode averaging — indispensable for long-distance part in isoQCD
- Four-dimensional stochastic sources at mass insertion



[Sebastian Lahrtz, PhD project]

Ensemble A654, 5000 configs, $m_\pi \simeq 330 \text{ MeV}$ $a \simeq 0.1 \text{ fm}$

Old setup: sequential propagator across mass insertion;
“spin-diluted” time slice sources (3D)

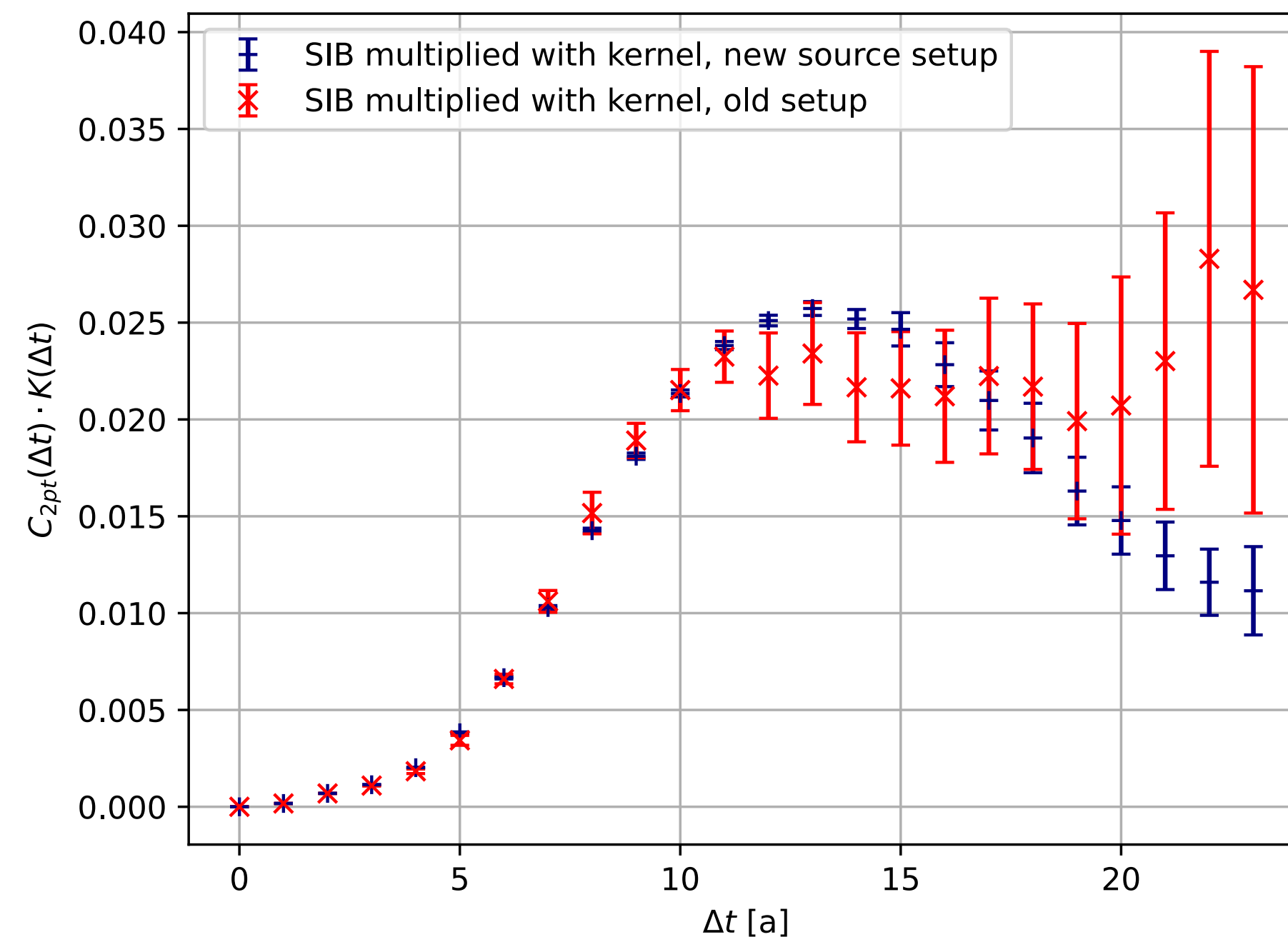
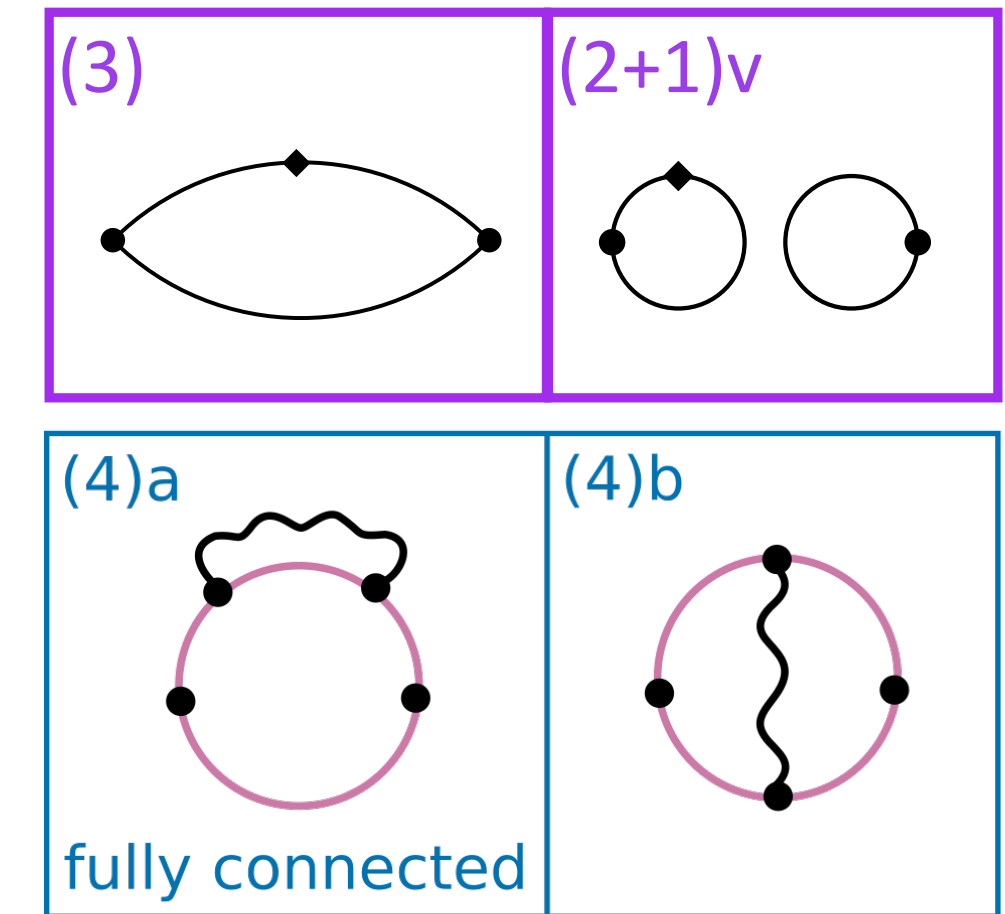
New setup: sequential propagator across vector current;
stochastic volume sources (4D);
compute (2+1)v diagram directly

Comparison for same numerical cost (# of inversions)

Isospin-breaking effects

Combat high levels of statistical noise in evaluation of mass insertion and fully connected QED diagrams using “Rome approach” and QED_L

- Low-mode averaging — indispensable for long-distance part in isoQCD
- Four-dimensional stochastic sources at mass insertion



[Sebastian Lohrtz, PhD project]

Ensemble A654, 5000 configs, $m_\pi \simeq 330 \text{ MeV}$ $a \simeq 0.1 \text{ fm}$

Old setup: sequential propagator across mass insertion;
“spin-diluted” time slice sources (3D)

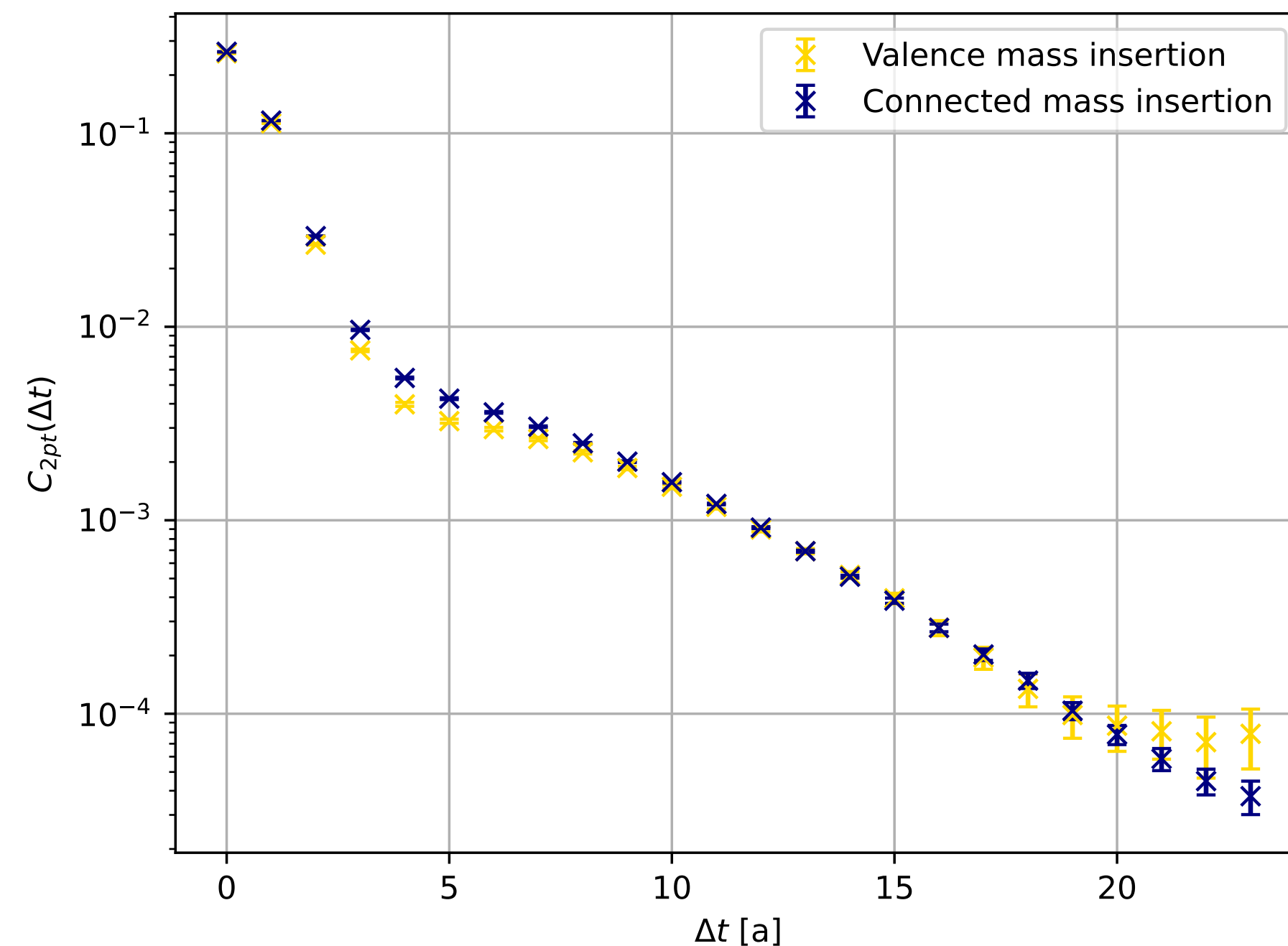
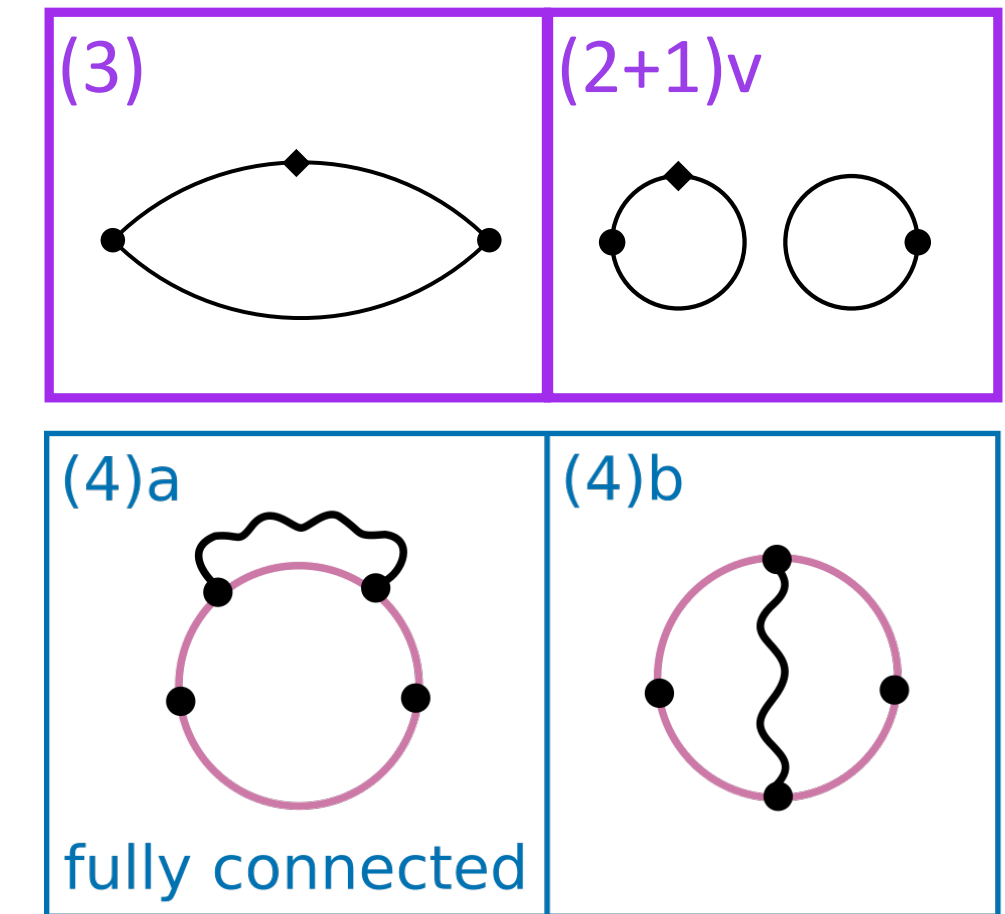
New setup: sequential propagator across vector current;
stochastic volume sources (4D);
compute (2+1)v diagram directly

Comparison for same numerical cost (# of inversions)

Isospin-breaking effects

Combat high levels of statistical noise in evaluation of mass insertion and fully connected QED diagrams using “Rome approach” and QED_L

- Low-mode averaging — indispensable for long-distance part in isoQCD
- Four-dimensional stochastic sources at mass insertion



[Sebastian Lahrtz, PhD project]

Ensemble A654, 5000 configs, $m_\pi \simeq 330 \text{ MeV}$ $a \simeq 0.1 \text{ fm}$

Old setup: sequential propagator across mass insertion;
“spin-diluted” time slice sources (3D)

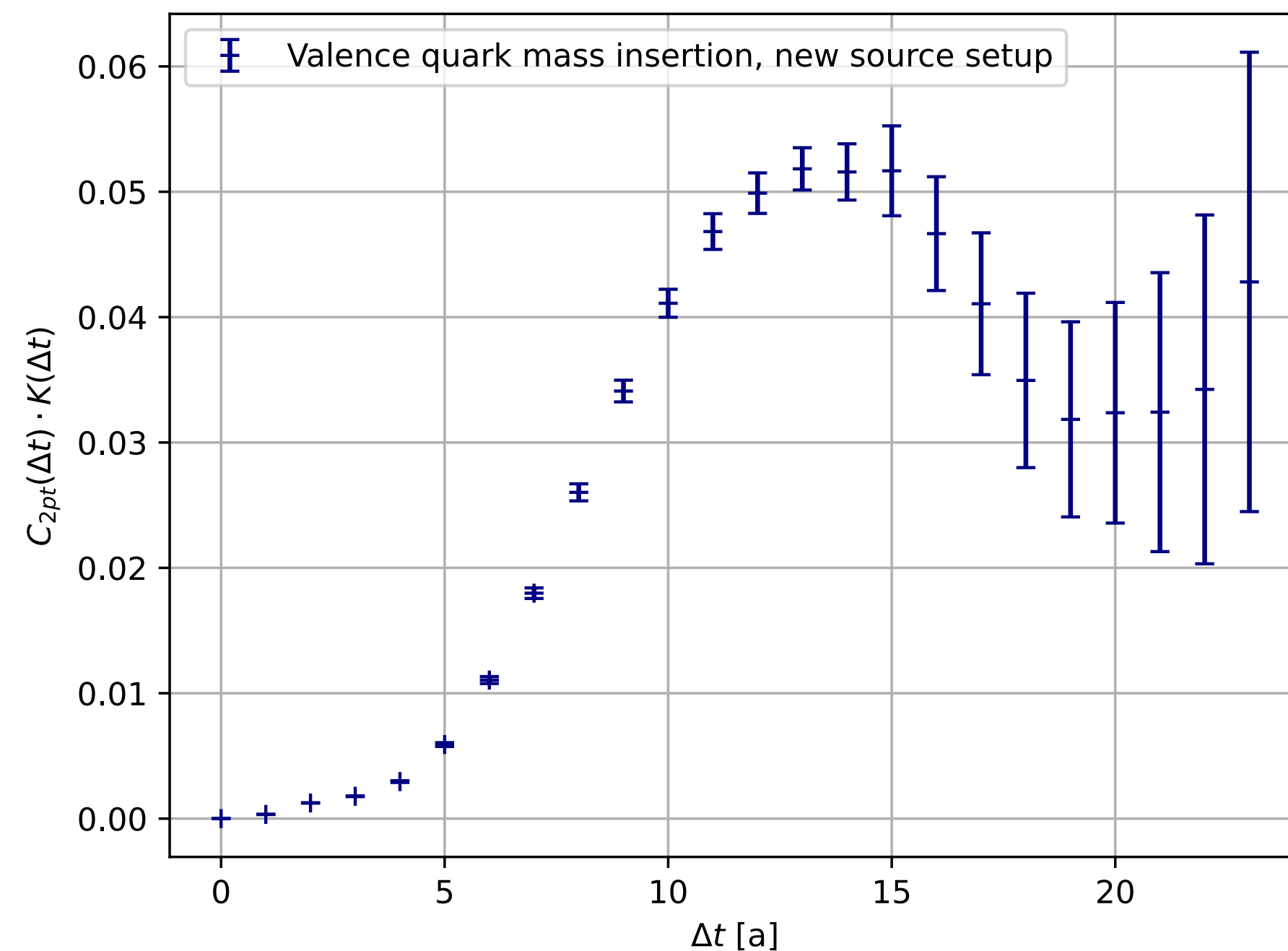
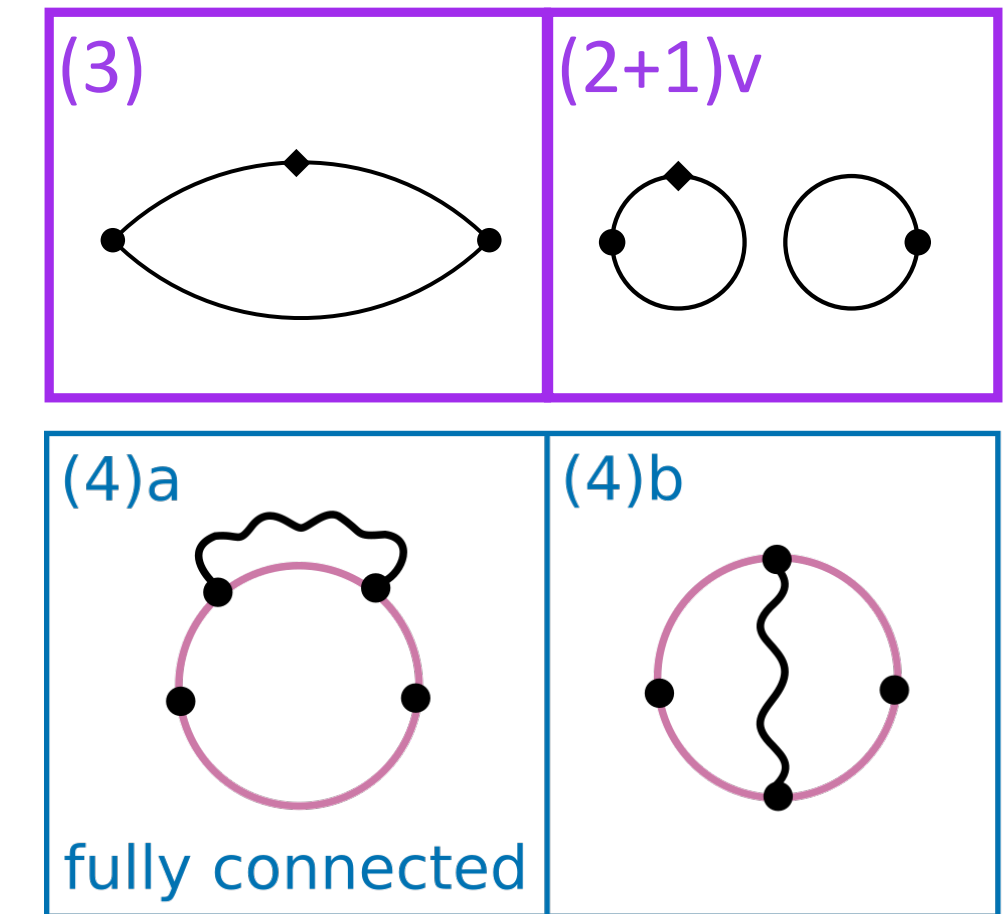
New setup: sequential propagator across vector current;
stochastic volume sources (4D);
compute (2+1)v diagram directly

Comparison for same numerical cost (# of inversions)

Isospin-breaking effects

Combat high levels of statistical noise in evaluation of mass insertion and fully connected QED diagrams using “Rome approach” and QED_L

- Low-mode averaging — indispensable for long-distance part in isoQCD
- Four-dimensional stochastic sources at mass insertion



[Sebastian Lahrtz, PhD project]

Ensemble A654, 5000 configs, $m_\pi \simeq 330 \text{ MeV}$ $a \simeq 0.1 \text{ fm}$

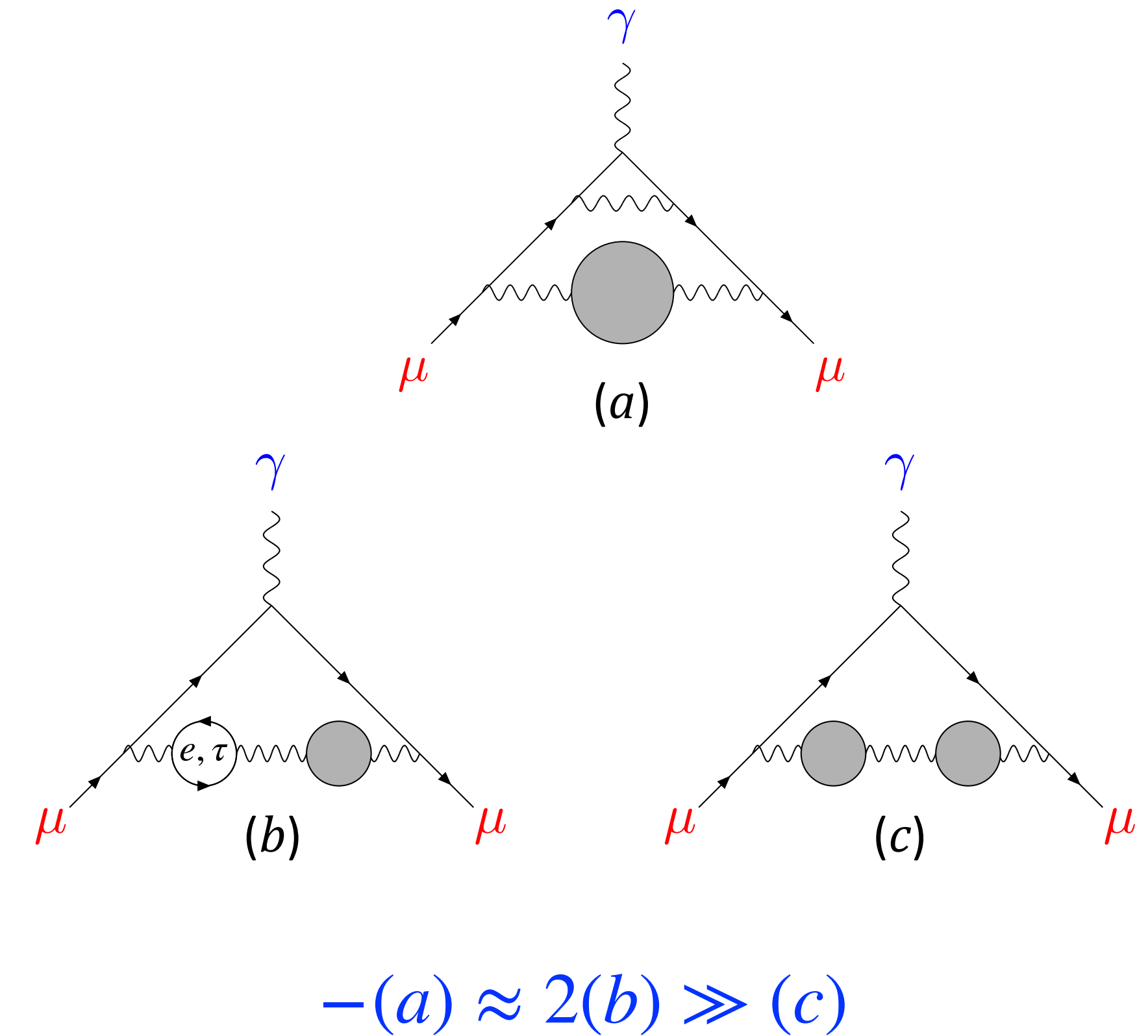
Old setup: sequential propagator across mass insertion;
“spin-diluted” time slice sources (3D)

New setup: sequential propagator across vector current;
stochastic volume sources (4D);
compute (2+1)v diagram directly

Comparison for same numerical cost (# of inversions)

Higher-order hadronic vacuum polarisation

| Contribution | Section | Equation | Value $\times 10^{11}$ | References |
|--|------------|------------|--------------------------------------|----------------------|
| Experiment (E989) | | Eq. (9.5) | 116 592 059(22) | Refs. [5–7, 9–12] |
| HVP LO (lattice) | Sec. 3.6.1 | Eq. (3.37) | 7132(61) | Refs. [13–29] |
| HVP LO (e^+e^- , τ) | Sec. 2 | Table 5 | Estimates not provided at this point | |
| HVP NLO (e^+e^-) | Sec. 2.9 | Eq. (2.47) | -99.6(1.3) | Refs. [30, 31] |
| HVP NNLO (e^+e^-) | Sec. 2.9 | Eq. (2.48) | 12.4(1) | Ref. [32] |
| HLbL (phenomenology) | Sec. 5.10 | Eq. (5.69) | 103.3(8.8) | Refs. [33–56] |
| HLbL NLO (phenomenology) | Sec. 5.10 | Eq. (5.70) | 2.6(6) | Ref. [57] |
| HLbL (lattice) | Sec. 6.2.8 | Eq. (6.34) | 122.5(9.0) | Refs. [58–62] |
| HLbL (phenomenology + lattice) | Sec. 9 | Eq. (9.2) | 112.6(9.6) | Refs. [33–56, 58–62] |
| QED | Sec. 7.5 | Eq. (7.27) | 116 584 718.8(2) | Refs. [63–69] |
| EW | Sec. 8 | Eq. (8.12) | 154.4(4) | Refs. [50, 70–72] |
| HVP LO (lattice) + HVP N(N)LO (e^+e^-) | Sec. 9 | Eq. (9.1) | 7045(61) | Refs. [13–32] |
| HLbL (phenomenology + lattice + NLO) | Sec. 9 | Eq. (9.3) | 115.5(9.9) | Refs. [33–62] |
| Total SM Value | Sec. 9 | Eq. (9.4) | 116 592 033(62) | Refs. [13–72] |
| Difference: $\Delta a_\mu \equiv a_\mu^{\text{exp}} - a_\mu^{\text{SM}}$ | Sec. 9 | Eq. (9.6) | 26(66) | |



NLO HVP arises at $O(\alpha^3)$; estimated using the data-driven method

Lattice calculation uses the same vector correlator $G(t)$ as input

Technical challenges similar to the LO HVP:

- statistical noise, disconnected diagrams, continuum limit, finite-volume effects, isospin breaking

Lattice approach to NLO HVP

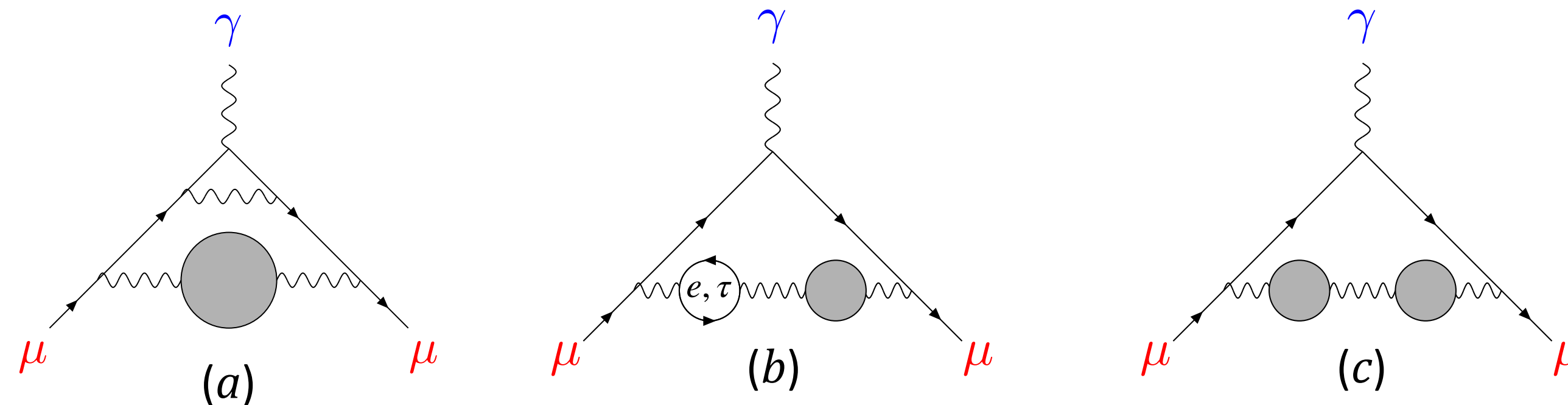
Adopt “Time-momentum representation” (TMR)

[Bernecker & Meyer, 2011]

Express NLO contributions in terms of convolution integrals of the spatially summed vector correlator

$$a_{\mu}^{\text{LO hvp}} = \left(\frac{\alpha}{\pi}\right)^2 \int_0^{\infty} dt \tilde{f}(t) G(t), \quad G(t) = -\frac{a^3}{3} \sum_k \sum_{\vec{x}} \langle j_k^{\text{em}}(\vec{x}, t) j_k^{\text{em}}(0) \rangle$$

$$a_{\mu}^{\text{NLO hvp}}[a, b] = \left(\frac{\alpha}{\pi}\right)^3 \int_0^{\infty} dt \tilde{f}[a, b](t) G(t), \quad a_{\mu}^{\text{NLO hvp}}[c] = \left(\frac{\alpha}{\pi}\right)^3 \int_0^{\infty} dt \int_0^{\infty} d\tau \tilde{f}[c](t, \tau) G(t) G(\tau)$$

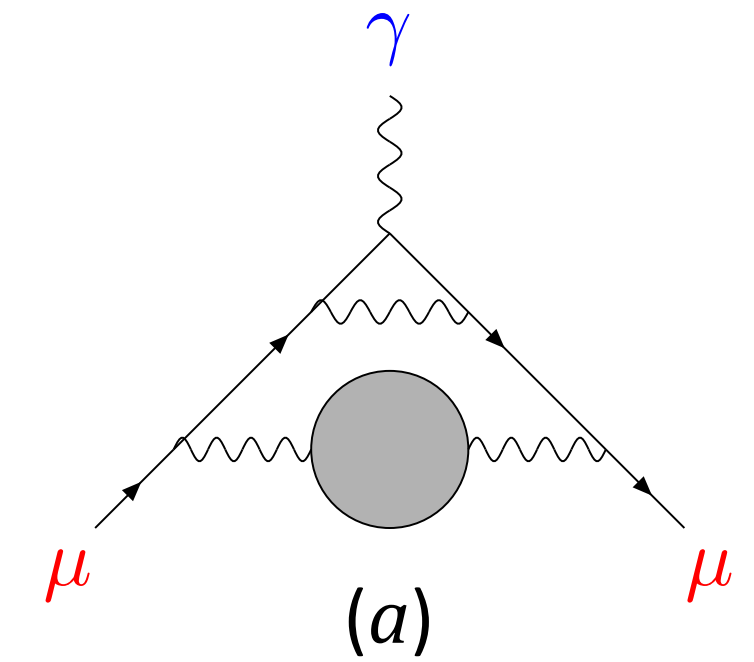


Work out kernel functions and find numerical representation with sufficient numerical precision

[Passera et al., PLB 834 (2022) 137462; Arnau Beltran Martínez, PhD project]

TMR kernel functions

Diagram (a)



NO closed-form solution.

$\hat{t} \ll 1$:

$$\int_0^\infty \frac{d\hat{\omega}^2}{\hat{\omega}^2} \hat{f}^{(\text{NLO}_a)}(\hat{\omega}^2) \left[\hat{\omega}^2 \hat{t}^2 - 4 \sin^2 \frac{\hat{\omega} \hat{t}}{2} \right] = \underbrace{\int_0^{\frac{1-\hat{t}}{\sqrt{\hat{t}}}} \frac{d\hat{\omega}^2}{\hat{\omega}^2} \hat{f}^{(\text{NLO}_a)}(\hat{\omega}^2) \left[\hat{\omega}^2 \hat{t}^2 - 4 \sin^2 \frac{\hat{\omega} \hat{t}}{2} \right]}_{\hat{\omega} \hat{t} \sim 0} + \int_{\frac{1-\hat{t}}{\sqrt{\hat{t}}}}^\infty \frac{d\hat{\omega}^2}{\hat{\omega}^2} \underbrace{\hat{f}^{(\text{NLO}_a)}(\hat{\omega}^2)}_{\hat{\omega} \sim \infty} \left[\hat{\omega}^2 \hat{t}^2 - 4 \sin^2 \frac{\hat{\omega} \hat{t}}{2} \right]$$

For $\hat{t} \gg 1$ one solves analytically as much as possible and rotates the cosine to the complex plane to make it real and thus make explicit the suppressed contribution. Then, one numerically expands around \hat{t}_0 by studying the asymptotic behavior of each piece.

Asymptotic expansions:

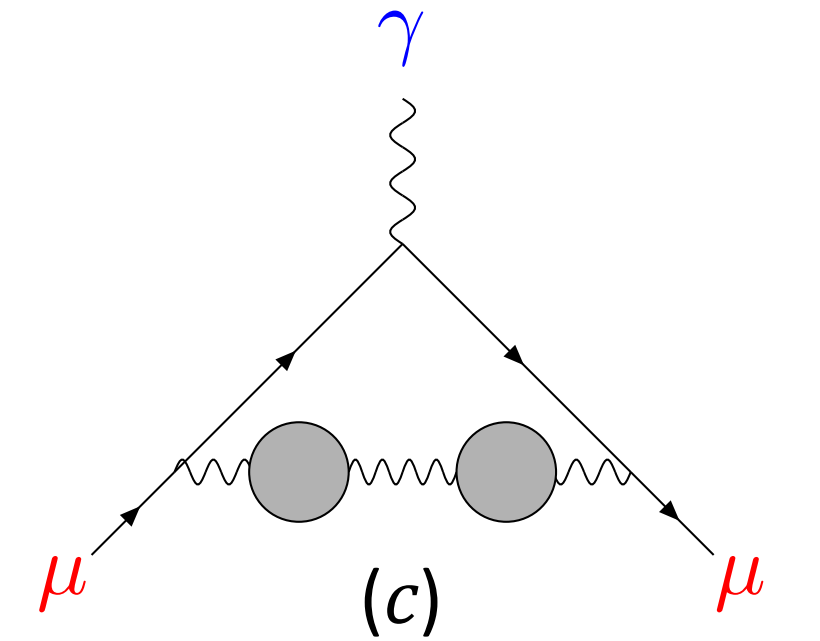
$$\frac{m_\mu^2}{16\pi^2} \tilde{f}^{\text{NLO}_a}(t) = \begin{cases} \sum_{n=4, n \in \text{even}}^N \frac{a_n + b_n \pi^2 + c_n (\gamma_E + \ln \hat{t}) + d_n (\gamma_E + \ln \hat{t})^2}{n!} \hat{t}^n & \hat{t} \leq \hat{t}^* \\ \text{Dominant}[\propto \hat{t}^2] + \sum_{p=0}^P \left[\left(\frac{a_p^{(b;1;1)}}{\hat{t}} + \frac{a_p^{(b;1;2)}}{\hat{t}^2} \right) \left(\frac{\hat{t}_0^2}{\hat{t}^2} - 1 \right)^p + e^{-2\hat{t}} \left(a_p^{(b;2;1)} + \frac{a_p^{(b;2;2)} \ln \hat{t} + a_p^{(b;2;3)}}{\sqrt{\hat{t}}} \right) \left(\frac{\hat{t}_0}{\hat{t}} - 1 \right)^p \right] & \hat{t} > \hat{t}^* \end{cases}$$

Ensure that numerical precision in representation of kernel function is better than $\lesssim 10^{-8}$

[Balzani, Laporta, Passera, PLB 858 (2024) 139040, Arnau Beltran Martínez, PhD project]

TMR kernel functions

Diagram (c)



Has a closed-form solution.

$$\begin{aligned}
 \frac{m_\mu^4}{32\pi^4} \tilde{f}^{(4c)}(\hat{t}, \hat{\tau}) &= \frac{\hat{\tau}^2 \hat{t}^2}{4} + \frac{\hat{t}^2}{\hat{\tau}^2} + \frac{\hat{\tau}^2}{\hat{t}^2} - \frac{1}{2}(\hat{t}^2 + \hat{\tau}^2) + \frac{1}{6} - 2(1 + \gamma_E) + 2\hat{t}^2(\ln \hat{\tau} + \gamma_E) + 2\hat{\tau}^2(\ln \hat{t} + \gamma_E) + 2(\hat{t}^2 - 1) \ln \hat{t} + 2(\hat{\tau}^2 - 1) \ln \hat{\tau} \\
 &+ [1 - (\hat{t} + \hat{\tau})^2] \ln(\hat{t} + \hat{\tau}) + [1 - (\hat{t} - \hat{\tau})^2] \ln|\hat{t} - \hat{\tau}| + \left(\frac{\hat{t}^2}{6} - 2\right) K_0(2\hat{t}) + \left(\frac{\hat{\tau}^2}{6} - 2\right) K_0(2\hat{\tau}) + \left(1 - \frac{1}{12}(\hat{t} + \hat{\tau})^2\right) K_0(2(\hat{t} + \hat{\tau})) + \left(1 - \frac{1}{12}(\hat{t} - \hat{\tau})^2\right) K_0(2|\hat{t} - \hat{\tau}|) \\
 &- \left(\frac{2\hat{t}^2}{\hat{\tau}} + \frac{\hat{\tau}}{12}\right) K_1(2\hat{\tau}) - \left(\frac{2\hat{\tau}^2}{\hat{t}} + \frac{\hat{t}}{12}\right) K_1(2\hat{t}) + \frac{1}{24}|\hat{t} - \hat{\tau}| K_1(2|\hat{t} - \hat{\tau}|) + \frac{1}{24}(\hat{t} + \hat{\tau}) K_1(2(\hat{t} + \hat{\tau})) + \left(\frac{\hat{t}^2}{12} + \frac{\hat{\tau}^2}{4} - \frac{15}{16}\right) G_{1,3}^{2,1} \left(\hat{t}^2 \left| \begin{matrix} \frac{3}{2} \\ 0, 1, \frac{1}{2} \end{matrix} \right. \right) \\
 &+ \left(\frac{\hat{\tau}^2}{12} + \frac{\hat{t}^2}{4} - \frac{15}{16}\right) G_{1,3}^{2,1} \left(\hat{\tau}^2 \left| \begin{matrix} \frac{3}{2} \\ 0, 1, \frac{1}{2} \end{matrix} \right. \right) + \left(\frac{15}{32} - \frac{1}{24}(\hat{t} + \hat{\tau})^2\right) G_{1,3}^{2,1} \left((\hat{t} + \hat{\tau})^2 \left| \begin{matrix} \frac{3}{2} \\ 0, 1, \frac{1}{2} \end{matrix} \right. \right) + \left(\frac{15}{32} - \frac{1}{24}(\hat{t} - \hat{\tau})^2\right) G_{1,3}^{2,1} \left((\hat{t} - \hat{\tau})^2 \left| \begin{matrix} \frac{3}{2} \\ 0, 1, \frac{1}{2} \end{matrix} \right. \right)
 \end{aligned}$$

Perform different asymptotic expansions depending on relative size of $\hat{t}, \hat{\tau}$

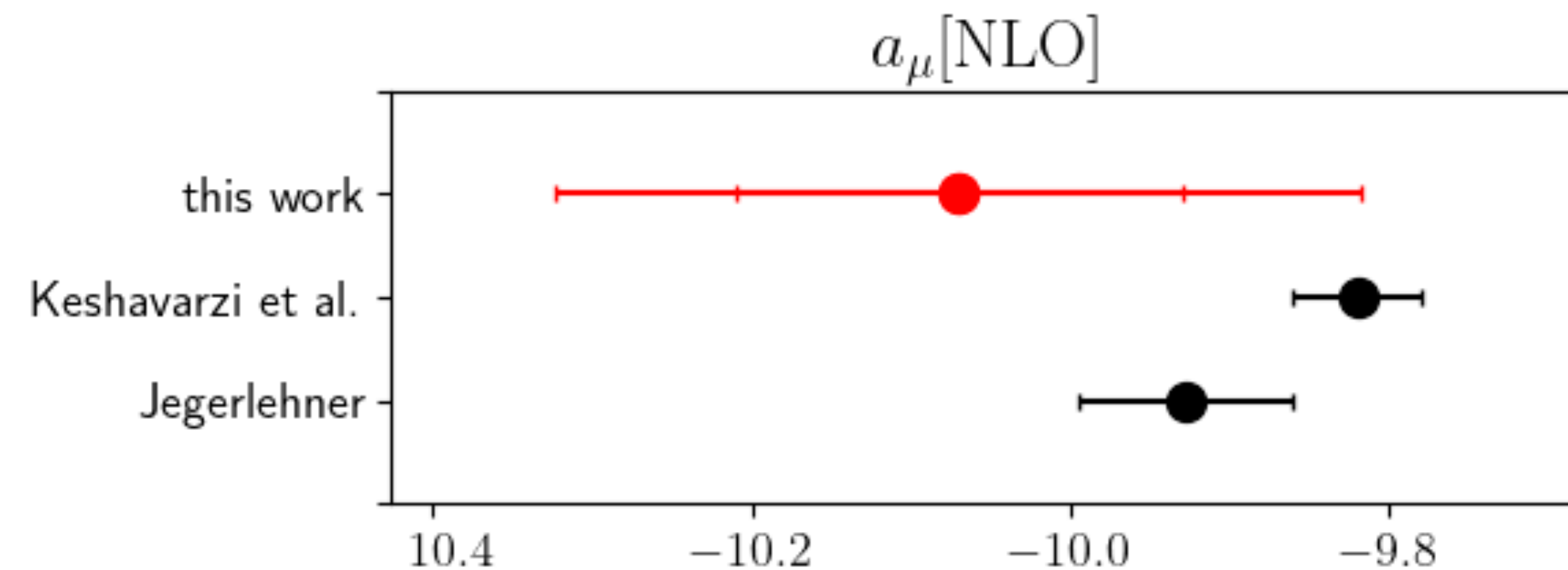
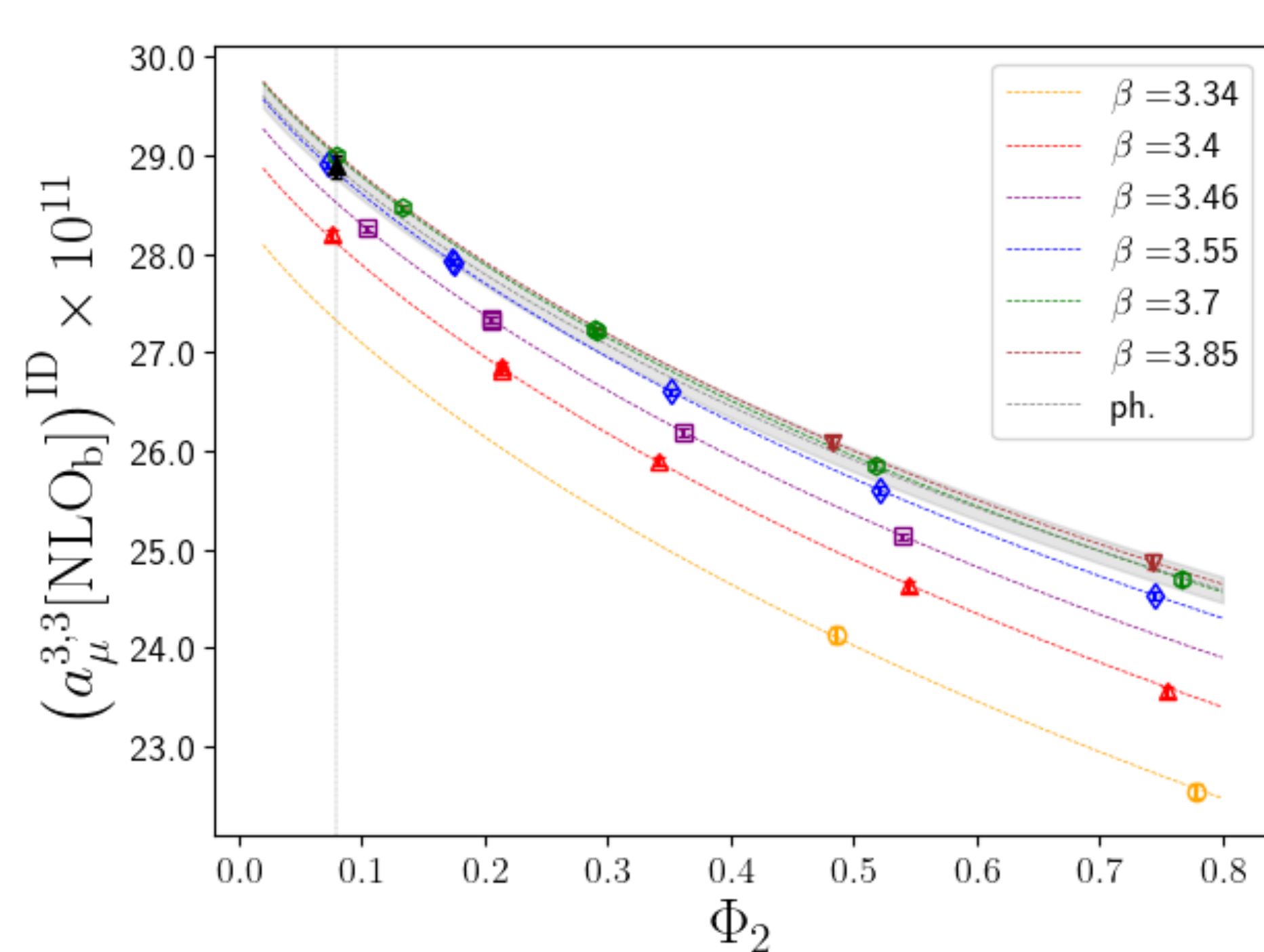
[Balzani, Laporta, Passera, PLB 858 (2024) 139040, Arnau Beltran Martínez, PhD project]

Preliminary results for NLO HVP contribution

Use subset of CLS ensembles

Compute diagrams (a)–(c) on each ensemble; correct for finite-volume effects

Perform chiral+continuum extrapolation; final result from model average



- Fully blinded analysis in progress
- Expect much higher statistical precision
- Include isospin-breaking corrections

[Balzani, Laporta, Passera, PLB 858 (2024) 139040, Arnau Beltran Martínez, PhD project]

(Interim) Conclusions

Strong and electromagnetic isospin breaking corrections crucial for improving precision of lattice-QCD calculations of the (LO) HVP contribution

Many technical challenges

- Statistical noise in diagrams containing mass insertions
- Complexity of set of diagrams

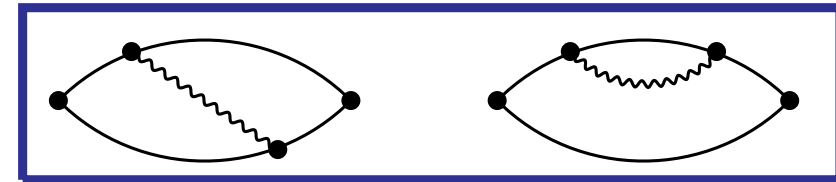
Mix of complementary methods crucial:

- Coordinate-space methods vs. QED_L
- Simulations of QCD with $N_f = 1 + 1 + 1$

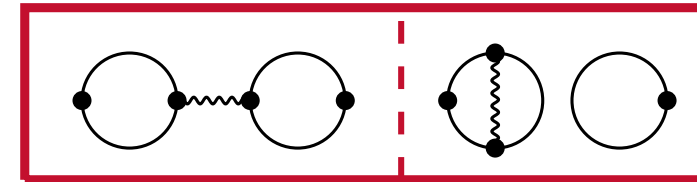
Good progress in calculating NLO HVP contribution in lattice QCD with competitive precision

Expect more precise updates on hadronic running of α and $\sin^2 \theta_W$

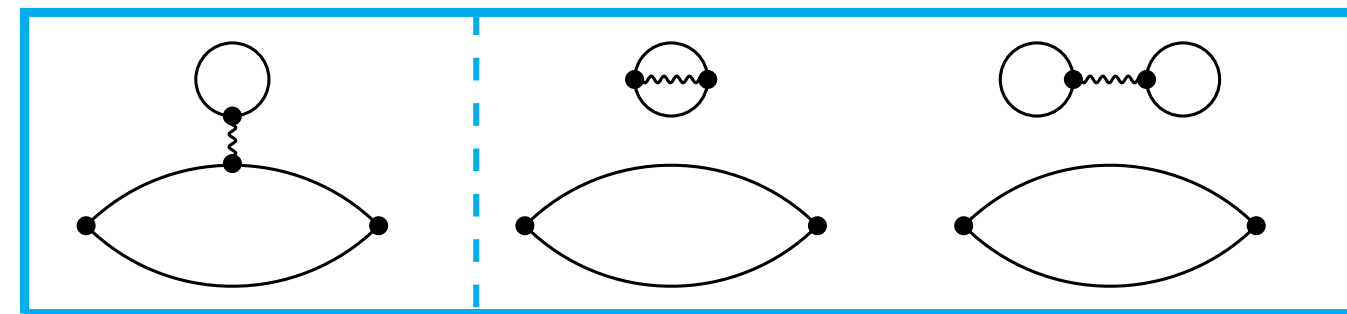
Isospin Breaking



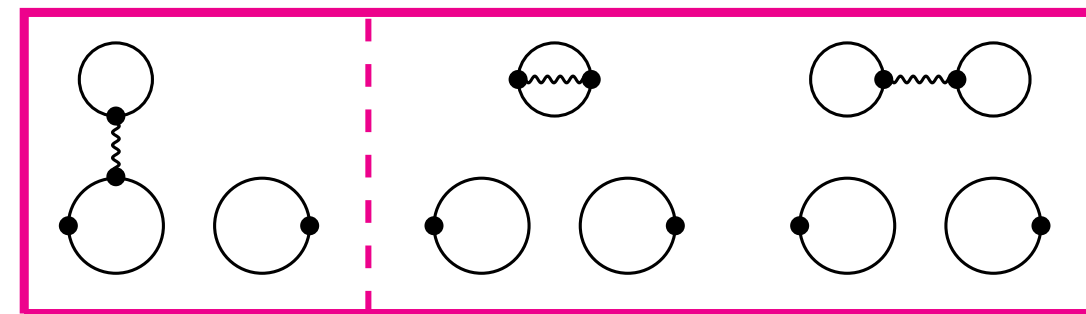
BMW $-1.27(40)(33)$
 RBC/UKQCD $5.9(5.7)(1.7)$
 ETM $1.1(1.0)$



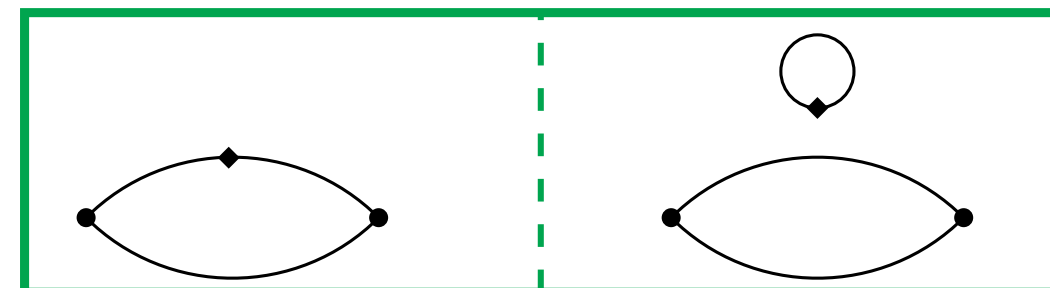
$-0.55(15)(11)$ BMW
 $-6.9(2.1)(2.0)$ RBC/UKQCD



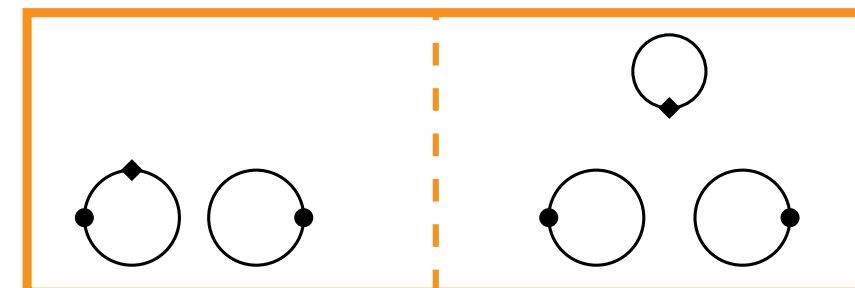
$-0.0095(86)(99)$ $0.42(20)(19)$ BMW



$0.011(24)(14)$ $-0.047(33)(23)$ BMW



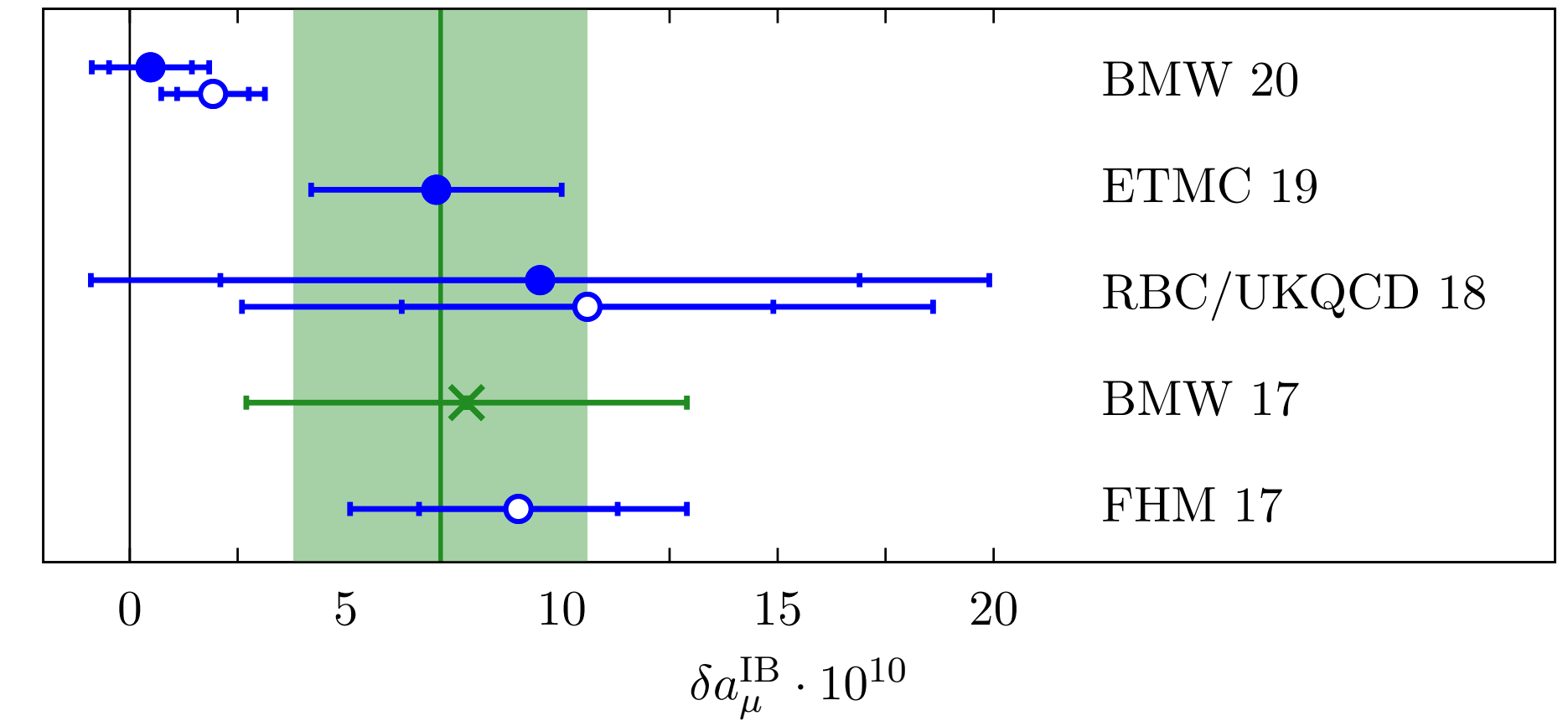
$6.59(63)(53)$ BMW
 $10.6(4.3)(6.8)$ RBC/UKQCD
 $6.0(2.3)$ ETM
 $7.7(3.7)$ $9.0(2.3)$ FHM
 $9.0(0.8)(1.2)$ LM



$-4.63(54)(69)$ BMW

BMW [arXiv:2002.12347]
 RBC/UKQCD [Phys.Rev.Lett. 121 (2018) 2, 022003]
 ETM [Phys. Rev. D 99, 114502 (2019)]
 FHM [Phys.Rev.Lett. 120 (2018) 15, 152001]
 LM [Phys.Rev.D 101 (2020) 074515]

Collection of published results:



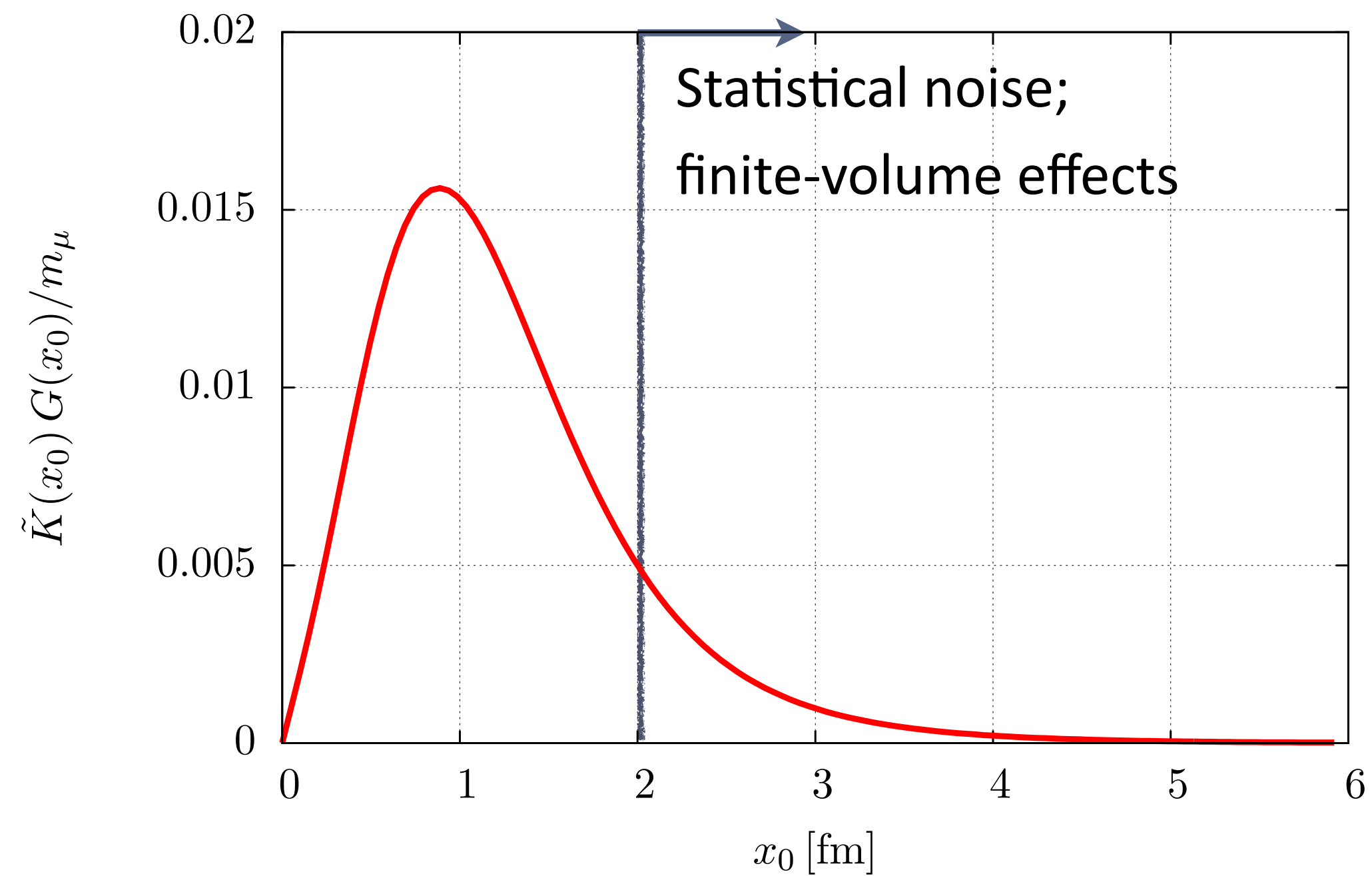
- Small overall value result of cancellations
- Large statistical uncertainties:

$$a_\mu^{\text{IB}} \lesssim 1\%, \quad \delta a_\mu^{\text{IB}} \lesssim 100\%$$
- More precise calculations required

(Compilation by Vera Gülpers, Lattice-HVP Workshop Nov 2020)

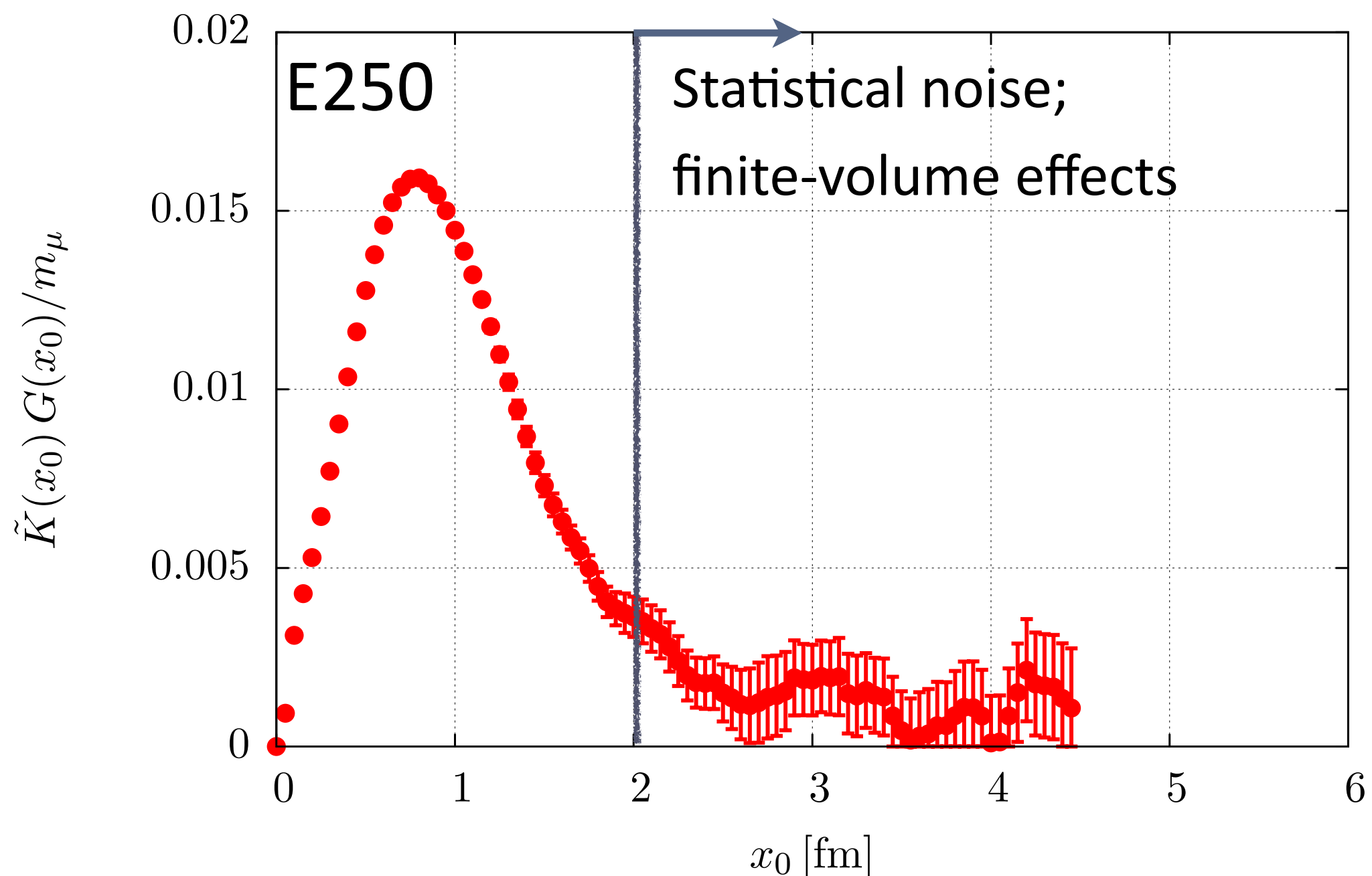
Noise-reduction strategies

Problem: exponential growth of signal-to-noise ratio in $G(t)$ for large t



Noise-reduction strategies

Problem: exponential growth of signal-to-noise ratio in $G(t)$ for large t



Noise-reduction technique: “Low-mode averaging” (LMA)

- Express quark propagator in terms of eigenmodes of the Wilson-Dirac operator

$$S(y, x) = S_{\text{eigen}}(y, x) + S_{\text{rest}}(y, x)$$

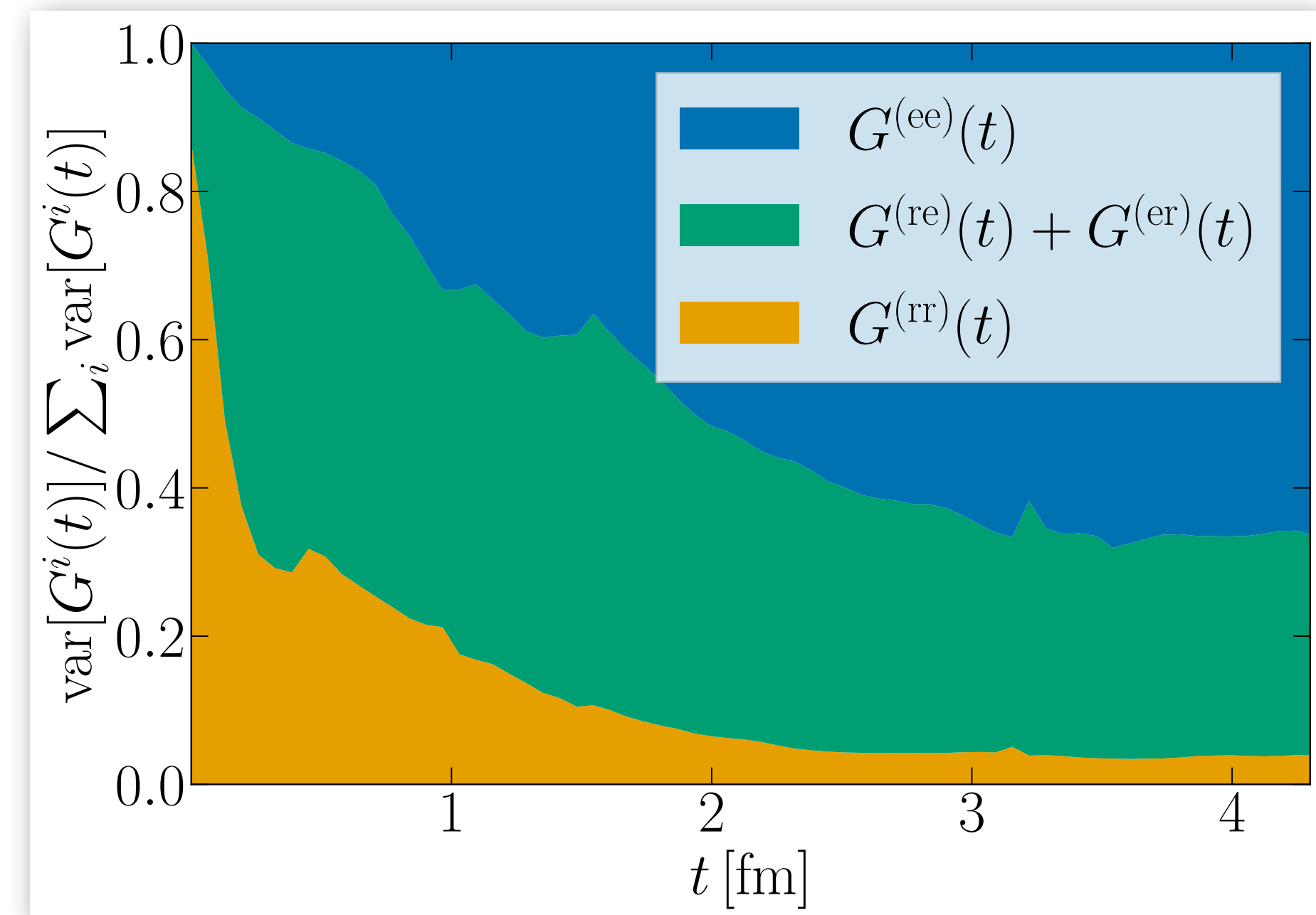
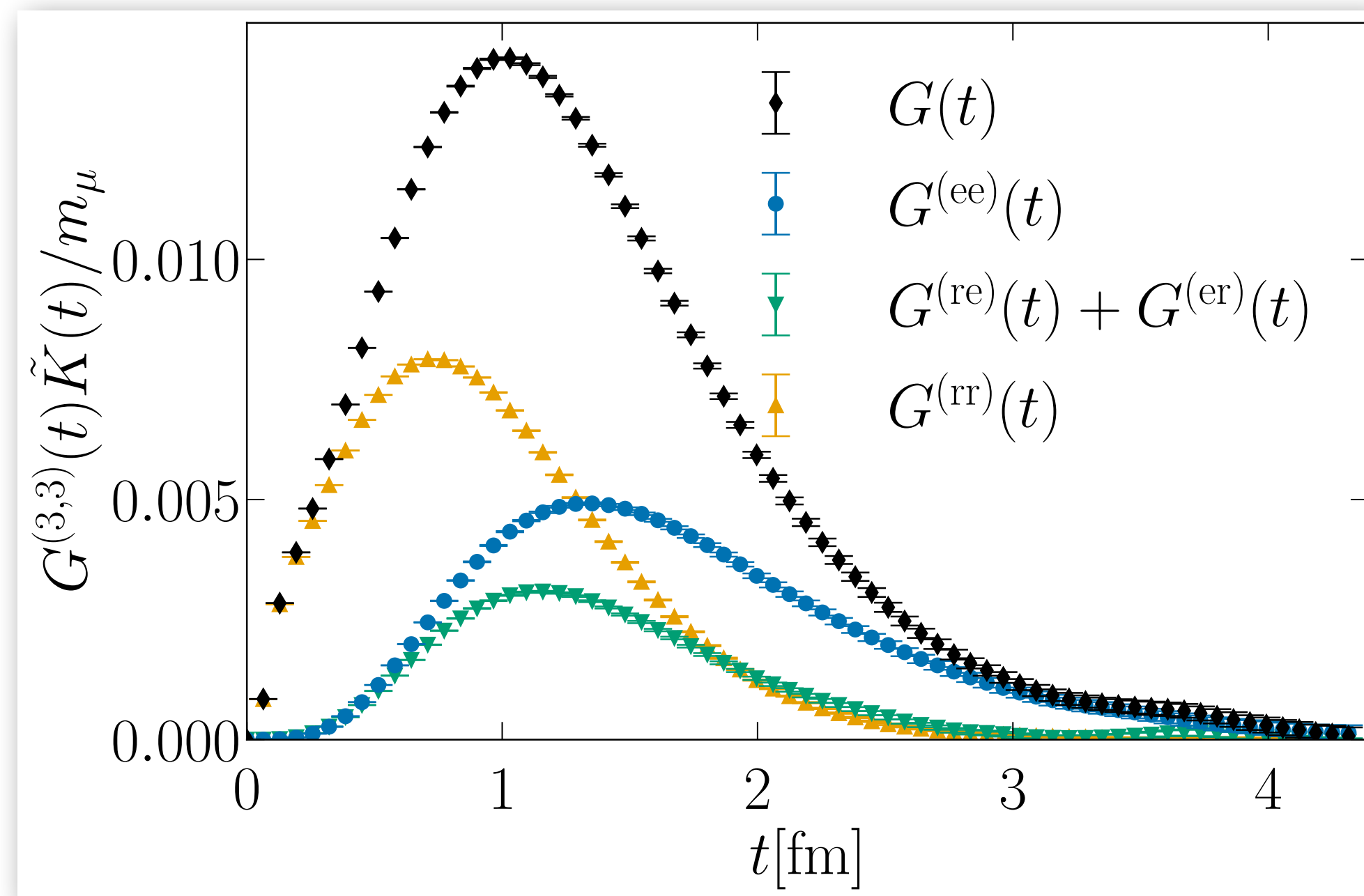
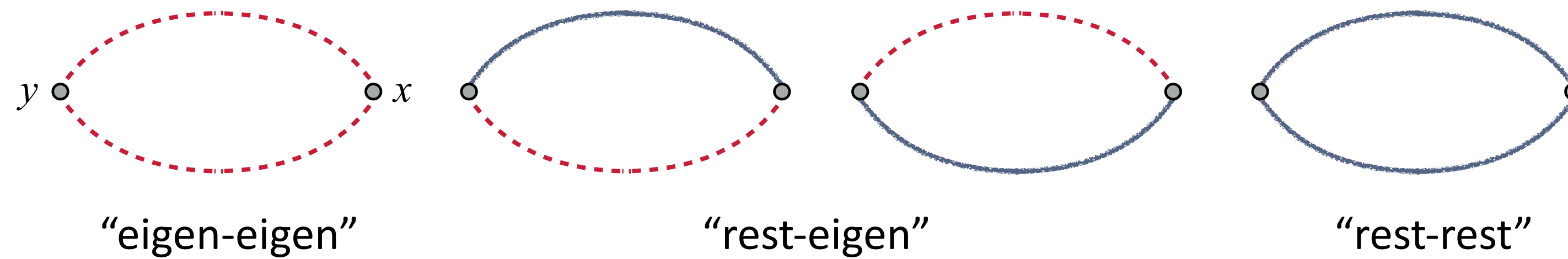
[Giusti, Hernández, Laine, Weisz, HW 2004; DeGrand & Schaefer 2004]

$$S_{\text{eigen}}(y, x) = \sum_{i=1}^{N_{\text{low}}} \lambda_i^{-1} v_i(x) \otimes (\gamma_5 v_i(y))^\dagger, \quad (\gamma_5 D_w) v_i(x) = \lambda_i v_i(x), \quad N_{\text{low}} \lesssim 1000$$

Low modes responsible for statistical fluctuations — LMA leads to better sampling of the correlator

Low-mode averaging

Compute and sum all combinations of low and high mode contributions to $G(t)$



Spectral reconstruction

Observation: long-distance regime of $G(t)$ dominated by two-pion states with isospin one

$$G(x_0) \stackrel{x_0 \rightarrow \infty}{=} \sum_n |A_n|^2 e^{-\omega_n t}$$

Strategy B:

- Perform a dedicated calculation of the spectrum of pion-pion states in the isovector channel
- Accumulate contributions from states $n = 0, 1, 2, \dots$ until saturation is observed

